arXiv:2412.03752v2 [cs.AI] 30 Mar 2025

Beyond Local Sharpness: Communication-Efficient Global Sharpness-aware Minimization for Federated Learning

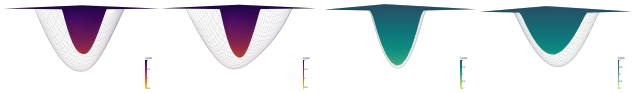
Debora Caldarola[1,*], Pietro Cagnasso[1], Barbara Caputo[1], Marco Ciccone[2,†]
[1]Politecnico di Torino, [2] Vector Institute

Abstract

Federated learning (FL) enables collaborative model training with privacy preservation. Data heterogeneity across edge devices (clients) can cause models to converge to sharp minima, negatively impacting generalization and robustness. Recent approaches use client-side sharpness-aware minimization (SAM) to encourage flatter minima, but the discrepancy between local and global loss landscapes often undermines their effectiveness, as optimizing for local sharpness does not ensure global flatness. This work introduces FEDGLOSS *(**Fed**erated **Glo**bal **S**erver-side **S**harpness), a novel FL approach that prioritizes the optimization of global sharpness on the server, using SAM. To reduce communication overhead,* FEDGLOSS *cleverly approximates sharpness using the previous global gradient, eliminating the need for additional client communication. Our extensive evaluations demonstrate that* FEDGLOSS *consistently achieves flatter minima and better performance compared to state-of-the-art FL methods in various federated vision benchmarks. Code available at github.com/pietrocagnasso/fedgloss.*

1. Introduction

Federated Learning (FL) [39] provides a powerful framework to collaboratively train machine learning models on private data distributed across multiple endpoints. Unlike traditional methods, FL enables edge devices (*clients*), like smartphones or IoT (Internet of Things) hardware, to train a shared model without compromising their sensitive information. This is achieved through communication rounds, where clients independently train on their local data and then exchange updated model parameters with a central server, preserving data privacy. The optimization on the server side relies on *pseudo-gradients* [47], *i.e.*, the average of the difference between the global model and the client's update, which serve as an estimate of the true global gradient on the overall dataset. This approach holds immense potential for privacy-sensitive applications, proving its value in areas like healthcare [2, 37, 41, 46], finance [41], autonomous driving [11, 40, 51], IoT [62], and more [32, 57]. However, the real-world deployment of FL presents unique challenges stemming from data heterogeneity and communication costs [34]. Clients gather their data influenced by various factors such as personal habits or geographical locations, leading to inherent differences across devices [20, 24, 51]. This results in the global model suffering from degraded performance and slower convergence [4, 25, 26, 36], with instability emerging as client-specific optimization paths diverge from the global one. This phenomenon, known as *client drift* [26], limits the model's ability to generalize to the overall underlying distribution.



(a) CIFAR10 $\alpha = 0$ (b) CIFAR10 $\alpha = 0.05$ (c) CIFAR100 $\alpha = 0$ (d) CIFAR100 $\alpha = 0.5$

Figure 1. Comparison of **FEDAVG** (*solid*) and **FEDSAM** (*net*) loss landscapes with varying degrees of data heterogeneity (α) on the CIFAR datasets. **FEDSAM's effectiveness in converging to *global* flat minima is highly influenced by the data heterogeneity**, where higher heterogeneity ($\alpha \to 0$) leads to sharper minima, and the complexity of the task, *e.g.*, higher sharpness for the more complex CIFAR100. This highlights the importance of optimizing global sharpness. Model: CNN.

While many FL approaches focus on mitigating client drift through client-side regularization [1, 35, 56], a recent trend leverages the geometry of the loss landscape to improve generalization [4, 7, 45, 53, 54]. These methods build upon the notion that convergence to sharp minima correlates with poor generalization [17, 23, 27]. FEDSAM [4, 45] employs Sharpness-aware Minimization (SAM) [12] in local training to guide clients toward flatter loss regions, enhancing global performance. This comes at the cost of increased client-side computation, since SAM requires two forward/backward passes for each local optimization step: a gradient ascent step to compute the maximum sharpness and a descent step for sharpness and loss value minimization. Although FEDSAM and its variants [7, 54] demonstrated their effectiveness in various settings, they rely solely on local flatness, assuming that minimizing sharpness

*Corresponding author: debora.caldarola@polito.it
†Work mainly carried out while at Politecnico di Torino

locally leads to a globally flat minimum[1]. However, in real-world scenarios with significant data heterogeneity, there can be substantial discrepancies between local and global loss landscapes and optimizing for local sharpness does not guarantee the global model will reside in a flat region (Fig. 1). Addressing these limitations, FEDSMOO [53] uses the alternating direction method of multipliers (ADMM) [3] to include global sharpness information in SAM's local training. While this approach reduces the inconsistency between local and global geometries, it increases communication costs by requiring double the bandwidth in each round. This hinders its real-world applicability, as FL relies on minimizing communication overhead (*i.e.*, message size and exchange frequency) to avoid network congestion and account for potential connection failures.

Given the limitations of existing methods, achieving global flat minima while ensuring communication efficiency in heterogeneous FL remains a critical challenge. To address this, we propose FEDGLOSS (**Fed**erated **Glo**bal **S**erver-side **S**harpness) that directly **optimizes global sharpness by using SAM on the server side**, avoiding additional exchanges over the network. Such adaptation is not straightforward, as SAM would require dual exchanges with each client set per round to solve its optimization problem. Instead, FEDGLOSS approximates the sharpness measure using available previous pseudo-gradients. As a result, it facilitates faster training and keeps communication efficiency. To summarize, our core contributions are the following:

- Empirical proof of local-global discrepancies: we provide the first empirical evidence showing the limitations of approaches that focus solely on local sharpness. Our analysis highlights the inconsistency between local and global loss geometries even when using sharpness-aware approaches like FEDSAM, demonstrating that local flatness does not necessarily ensure a flat global minimum. While reaching flat global solutions in simpler problems, we show that their effectiveness diminishes as data complexity and heterogeneity increase (Fig. 1).
- To bridge this gap and motivated by communication efficiency, our FEDGLOSS algorithm directly optimizes for global sharpness on the server using SAM, reducing the communication overhead and the clients' computational costs compared to previous works. FEDGLOSS consistently achieves flatter minima and outperforms state-of-the-art methods across various vision benchmarks.
- We show the importance of aligning global and local solutions and illustrate how SAM, especially on the server side, enables effective ADMM use in FL. While typically ADMM-based methods suffer from parameter explosion [56], we show that by targeting flat minima, SAM encourages smaller gradient steps and minimal weight updates, leading to a significantly more stable algorithm.

[1]We use the term "global flat minima" to refer to local minima within the global (*i.e.*, server-side) loss landscape.

2. Related works

Federated framework. In the last few years, Federated Learning (FL) [39] garnered significant attention from both the machine learning and computer vision communities. While the former has primarily focused on optimizing FL algorithms and guaranteeing their convergence [1, 36, 47], the latter has explored its applications in real-world settings, spanning diverse domains like autonomous driving [11, 40, 51] and healthcare [37]. The key appeal of FL lies in its ability to efficiently learn from privacy-protected, distributed data while complying with regulations and leveraging edge resources. Real-world deployments of FL range across both *cross-silo* and *cross-device* settings [24]. This work focuses on the latter, with up to millions of individual devices at the network edge, with typically limited data and computational power, and potential unavailability due to battery life or network connectivity issues. User-specific factors like geographical location, capturing devices and daily habits introduce inherent *bias* and *statistical heterogeneity* into the local datasets. In this setting, FEDGLOSS aims to learn a global model that generalizes to the overall data distribution under statistical heterogeneity without increasing communication complexity, unlike other algorithms for local-global consistency in heterogeneous FL.

Flatness search in FL. Recent research has explored the connection between loss landscape geometry and generalization in heterogeneous FL. Studies suggest that convergence to sharp minima might hinder generalization performance [17, 27, 44]. SAM (Sharpness-Aware Minimization) [12] tackles this issue by guiding the optimization toward flatter regions, seeking minima that exhibit both low loss and low sharpness. FEDSAM [4, 45] deploys SAM in local training, marking the first step toward leveraging loss surface geometry in FL to reduce discrepancies between local and global objectives, ultimately improving the global model's generalization ability. Following its success, FEDSPEED [54] uses perturbed gradients as SAM to reduce local overfitting, FEDGAMMA [7] combines the stochastic variance reduction of SCAFFOLD with SAM and Shi et al. [52] show FEDSAM's effectiveness in mitigating the negative effects of differential privacy. However, these approaches rely on *local* sharpness information, assuming its minimization directly translates to a globally flat minimum. This may not always be true, as we hypothesize discrepancies may exist between the geometries of local and global losses. Optimizing local sharpness alone does not guarantee a server model residing in a flat region of the *global* loss landscape (Fig. 1). Addressing these limitations, FEDSMOO [53] applies ADMM [3] to the sharpness measure to enforce global and local consistency. This adds communication overhead, doubling the message size in each round and hindering its

real-world practicality. In contrast, our work focuses on minimizing global sharpness while maintaining communication efficiency. Lastly, building on Stochastic Weight Averaging [22], other works [4, 5] use a window-based average of global models across rounds to reach wider minima. Being agnostic to the underlying optimization algorithm, they remain orthogonal to our approach.

Heterogeneity in FL. The de-facto standard algorithm for FL is FEDAVG [39], which updates the global model with a weighted average of the clients' parameters. However, FEDAVG struggles when faced with heterogeneous data distributions, leading to performance degradation and slow convergence due to the local optimization paths diverging from the global one [26]. Reddi et al. [47] shows FEDAVG is equivalent to applying Stochastic Gradient Descent (SGD) [49] with a unitary learning rate on the server side, using the difference between the initial global model parameters and the clients' updates as *pseudo-gradient*, opening the door to alternative optimizers beyond SGD to improve performance and convergence speed. Building on this intuition, this work proposes SAM [12] as a server-side optimizer to enhance generalization by converging toward *global* flat minima. Since SAM requires two optimization steps per iteration, a direct adaptation to the FL setting would double communication exchanges between clients and server; FEDGLOSS overcomes this limitation and maintains communication efficiency through the use of the latest pseudo-gradient as sharpness approximation.

Several approaches address client drift by adding regularization during local training. FedProx [35] introduces a term to keep local parameters close to the global model, FEDDYN [1] employs ADMM to align local and global convergence points, ADABEST [56] adjusts local updates with an adaptive bias estimate, and SCAFFOLD [26] applies stochastic variance reduction. Momentum-based techniques [55] are also employed to maintain a consistent global trajectory, either on the server side (*e.g.*, FEDAVGM [19]) or by incorporating global information into local training [13, 25, 28, 61]. Unlike FEDDYN, where ADMM can lead to parameter explosion [56], our FEDGLOSS successfully leverages ADMM to align global and local solutions, even under extreme heterogeneity, aided by SAM on server.

Centralized SAM. To avoid doubling client-server exchanges caused by SAM's two-step process, FEDGLOSS draws on insights from the literature on SAM in centralized settings. Several strategies have been proposed to minimize computational overhead, including reducing the number of parameters needed to compute the sharpness-aware components [9], or approximating them [10, 38, 42]. DP-SAT [42] approximates the ascent step with the gradient from the previous iteration, and SAF [10] replaces SAM's sharpness approximation with the trajectory of weights learned during training. Aiming to the same goal, FEDGLOSS approximates the sharpness measure with the pseudo-gradient from the previous round on the server side, without incurring in unnecessary exchanges with the clients and effectively guiding the optimization toward globally flat minima.

3. Background

This section introduces the FL problem setting and preliminary notations on SAM [12] and FEDSAM [4, 45].

3.1. Problem setting

In FL, a central server communicates with a set of clients $\mathcal{C}$ for T rounds. The goal is to learn a global model $f(\boldsymbol{w}) : \mathcal{X} \to \mathcal{Y}$ parametrized by $\boldsymbol{w} \in \mathbb{R}^d$, where $\mathcal{X}$ and $\mathcal{Y}$ are the input and the output spaces respectively. In image classification, $\mathcal{X}$ contains the images and $\mathcal{Y}$ their corresponding labels. Each client $k \in \mathcal{C}$ has access to a local dataset $\mathcal{D}_k$ of N_k pairs $\{(x_i, y_i), x_i \in \mathcal{X}, y_i \in \mathcal{Y}\}_{i=1}^{N_k}$. In realistic heterogeneous settings, clients usually hold different data distributions and quantity, *i.e.*, $D_i \neq D_j$ and $N_i \neq N_j \, \forall i \neq j \in \mathcal{C}$. The global FL objective is:

$$\min_{\boldsymbol{w}} \left\{ f(\boldsymbol{w}) = \frac{1}{C} \sum_{k \in \mathcal{C}} f_k(\boldsymbol{w}) \right\}, f_k(\boldsymbol{w}) \triangleq \mathbb{E} f_k(\boldsymbol{w}, \xi_k), \quad (1)$$

where $C \triangleq |\,\mathcal{C}\,|$ is the total number of clients, f_k is the empirical loss on the k-th client (*e.g.*, cross-entropy loss) and ξ_k is the data sample randomly drawn from the local data distribution D_k. The training process is a two-phase optimization approach within each round $t \in [T]$. First, due to potential client unavailability, a subset of selected clients $\mathcal{C}^t \subset \mathcal{C}$ trains the received global model using their local optimizer CLIENTOPT (*e.g.*, SGD, SAM). Then, the server aggregates their updates with a server optimizer, SERVEROPT. FEDOPT [47] solves Eq. (1) as

$$\Delta_{\boldsymbol{w}}^t \triangleq \sum_{k \in \mathcal{C}^t} \frac{N_k}{N} (\boldsymbol{w}^t - \boldsymbol{w}_k^t) \text{ and} \quad (2)$$

$$\boldsymbol{w}^{t+1} \leftarrow \boldsymbol{w}^t - \text{SERVEROPT}(\boldsymbol{w}^t, \Delta_{\boldsymbol{w}}^t, \eta_s), \quad (3)$$

where $\Delta_{\boldsymbol{w}}^t$ is the **global pseudo-gradient** at round t, $N = \sum_{k \in \mathcal{C}^t} N_k$ the total number of images seen during the current round, η_s the server learning rate, $\boldsymbol{w}^t$ the global model and $\boldsymbol{w}_k^t$ the local update resulting from training on client k's data with CLIENTOPT for E epochs. FEDAVG [39] computes $\boldsymbol{w}^{t+1}$ as $\sum_{k \in \mathcal{C}^t} {}^{N_k}\!/_N \, \boldsymbol{w}_k^t$, corresponding to one SGD step on the pseudo-gradient $\Delta_{\boldsymbol{w}}^t$ with $\eta_s = 1$ [47].

3.2. Sharpness-aware Minimization

SAM [12] jointly minimizes the loss value and the sharpness of the loss landscape by solving the min-max problem

$$\min_{\boldsymbol{w}} \left\{ F(\boldsymbol{w}) \triangleq \max_{\|\boldsymbol{\epsilon}\| \leq \rho} f(\boldsymbol{w} + \boldsymbol{\epsilon}) \right\}, \quad (4)$$

where $\boldsymbol{\epsilon}$ is the perturbation to estimate the sharpness, f the loss function, ρ the neighborhood size and $\|\cdot\|$ the ℓ_2 norm.

Using the first-order Taylor expansion of f, SAM efficiently solves the inner maximization as

$$\underset{\|\boldsymbol{\epsilon}\|\leq\rho}{\operatorname{argmax}} f(\boldsymbol{w})+\boldsymbol{\epsilon}^\top \nabla_{\boldsymbol{w}} f(\boldsymbol{w}) = \rho\frac{\nabla_{\boldsymbol{w}} f(\boldsymbol{w})}{\|\nabla_{\boldsymbol{w}} f(\boldsymbol{w})\|} \triangleq \hat{\boldsymbol{\epsilon}}(\boldsymbol{w}). \quad (5)$$

$\hat{\boldsymbol{\epsilon}}$ is the scaled gradient of the loss w.r.t. the current parameters $\boldsymbol{w}$. The *sharpness-aware gradient* is $\nabla_{\boldsymbol{w}} f(\boldsymbol{w})|_{\boldsymbol{w}+\hat{\boldsymbol{\epsilon}}(\boldsymbol{w})}$. Eq. (4) is solved with a first gradient ascent step to compute $\hat{\boldsymbol{\epsilon}}$ and a descent step with the sharpness-aware gradient, updating the model as $\boldsymbol{w} \leftarrow \boldsymbol{w} - \eta \nabla_{\boldsymbol{w}} f(\boldsymbol{w})|_{\boldsymbol{w}+\hat{\boldsymbol{\epsilon}}(\boldsymbol{w})}$.

3.3. SAM in Federated Learning

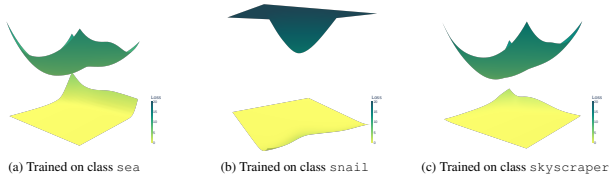
FEDSAM [4, 45] aims to improve the clients' models generalization through convergence to flatter regions by using SAM in the local training. From Eqs. (1) and (4), the global objective becomes $\min_{\boldsymbol{w}} \left\{ f^{\text{SAM}}(\boldsymbol{w}) = 1/C \sum_{k\in\mathcal{C}} f_k^{\text{SAM}}(\boldsymbol{w}) \right\}$, with $f_k^{\text{SAM}}(\boldsymbol{w}) \triangleq \max_{\|\boldsymbol{\epsilon}_k\|\leq\rho} f_k(\boldsymbol{w}+\boldsymbol{\epsilon}_k)$ with local perturbation $\boldsymbol{\epsilon}_k$. The intuition behind this approach is that the improved local models' generalization positively reflects on the global model performance. However, by independently applying Eq. (4) in the local optimization, FEDSAM does not explicitly address global flatness, potentially leading to discrepancies between local and global loss geometries.

4. Local-Global Sharpness Inconsistency

This section empirically investigates the hypothesis that discrepancies between local and global loss landscapes impact FEDSAM's performance, using a CNN model on CIFAR10 and CIFAR100 datasets — further details in Sec. 6.

Fig. 1 compares the loss surfaces of CNNs trained with FEDAVG and FEDSAM. On the easier CIFAR10, FEDSAM exhibits flatter minima w.r.t. FEDAVG, effectively navigating simpler landscapes. However, their difference diminishes with increasing dataset complexity (CIFAR100) and heterogeneity ($\alpha \to 0$). This suggests larger discrepancies between local and global geometries arise as tasks become more complex and data distributions more diverse.

To highlight the existing difference between local and global behavior, Fig. 2 investigates the behavior of client models at the end of local training when tested on their own data $\mathcal{D}_k$ (*bottom* landscape), prior to server-side aggregation, w.r.t. the overall dataset $\mathcal{D}$ (*top* landscape). Each plot shows the behavior of one of the randomly selected clients during the last round with FEDSAM, distinguished by the locally seen class (results for all 5 clients in App. B). The inconsistency between local and global behavior can be easily appreciated: locally, each model lands in a flat region; differently, the same model is close to saddle points (Fig. 2a) or sharp minima (Figs. 2b and 2c) in the global landscape. These findings are further corroborated by the maximum Hessian eigenvalues presented in Tab. 1, computed using each client's local dataset ($\lambda_{1,l}$) and the overall one ($\lambda_{1,g}$). FEDSAM performs well on simple datasets like CIFAR10



(a) Trained on class `sea` (b) Trained on class `snail` (c) Trained on class `skyscraper`

Figure 2. **Global *vs.* local perspective on FEDSAM.** CIFAR100 $\alpha = 0$ @ $20k$ rounds on CNN. Local models trained on one `class`, tested on the local (*bottom landscape*) or global dataset (*top landscape*). **Models trained with FEDSAM present significant differences between local and global behaviors.**

Table 1. **Maximum Hessian eigenvalues of local models**, computed on global ($\lambda_{1,g}$) and local datasets ($\lambda_{1,l}$). CIFAR10 and CIFAR100, $\alpha = 0$. Each client is identified via its local class. The lowest $\lambda_{1,g}$ in **bold**. FEDDYN does not converge on CIFAR100 with $\alpha = 0$ [4, 56], hence the lack of results (✗).

	Local Class	FEDAVG		FEDSAM		FEDDYN		FEDDYN + SAM		FEDSMOO		FEDGLOSS	
		$\lambda_{1,l}$	$\lambda_{1,g}$	$\lambda_{1,l}$	$\lambda_{1,g}$	$\lambda_{1,l}$	$\lambda_{1,g}$	$\lambda_{1,l}$	$\lambda_{1,g}$	$\lambda_{1,l}$	$\lambda_{1,g}$	$\lambda_{1,l}$	$\lambda_{1,g}$
CIFAR10	airplane	9.1	239.1	100.6	36.4	752.5	347.8	199.6	12.0	122.1	26.5	190.1	**4.3**
	cat	424.2	273.6	28.8	16.5	59.9	242.3	122.0	11.1	82.4	26.9	106.9	**3.9**
	bird	18.4	237.0	106.4	35.7	894.0	371.2	200.2	12.0	134.2	25.7	200.1	**4.1**
	airplane	483.5	269.5	103.2	30.6	761.6	348.9	206.9	12.3	122.8	25.2	207.8	**4.0**
	frog	263.2	259.6	68.1	32.9	528.9	286.0	155.6	11.7	79.3	33.5	84.8	**4.1**
CIFAR100	sea	251.0	224.5	0.1	238.5					33.2	31.4	28.3	**19.6**
	snail	91.2	267.0	0.2	149.1					331.2	102.2	260.8	**40.7**
	bear	108.4	215.2	6.7	129.3	✗	✗	✗	✗	428.6	121.0	220.3	**49.6**
	skyscraper	613.3	300.1	1.3	194.6					143.5	40.2	269.2	**22.2**
	possum	37.9	259.6	15.3	142.6					455.5	90.9	392.4	**39.0**

with global eigenvalues smaller than local ones. However, $\lambda_{1,l} \ll \lambda_{1,g}$ on the more complex CIFAR100. This suggests that FEDSAM effectively achieves *local* convergence to flatter regions of the loss landscape on individual devices, but the higher global eigenvalue indicates limitations in reaching a *globally* flat minimum. The challenge of achieving flat regions under high heterogeneity and the gap between local and global flatness support the introduction of FEDGLOSS.

5. FL with Global Server-side Sharpness

FEDGLOSS (Federated Global Server-side Sharpness) overcomes FEDSAM's limitations by efficiently optimizing both global flatness and consistency.

5.1. Rethinking SAM in Federated Learning

Aiming to optimize SAM's objective (Eq. (4)) on the global function, FEDGLOSS solves $\min_{\boldsymbol{w}} \left\{ \mathcal{F}(\boldsymbol{w}) = \frac{1}{C} \sum_{k\in\mathcal{C}} \mathcal{F}_k(\boldsymbol{w}) \right\}$, with $\mathcal{F}_k(\boldsymbol{w}) \triangleq \max_{\|\boldsymbol{\epsilon}\|\leq\rho} f_k(\boldsymbol{w}+\boldsymbol{\epsilon})$, where $\boldsymbol{\epsilon}$ is the global perturbation. Calculating the true $\boldsymbol{\epsilon}$ value requires the global gradient $\nabla_{\boldsymbol{w}} f$ (Eq. (5)) computed on the entire dataset $\mathcal{D} \triangleq \cup_{k\in\mathcal{C}} \mathcal{D}_k$, which is not available in FL due to data privacy and communication constraints. While FEDSMOO [53] tackles this issue by using ADMM on the sharpness with the constraint $\boldsymbol{\epsilon} = \boldsymbol{\epsilon}_k$, it necessitates transmitting $\boldsymbol{\epsilon}$ alongside the model parameters $\boldsymbol{w}$ to both clients and server in each round, hindering its practicality in real-world scenarios with limited communication budgets. This observation motivates the question: *how to minimize global sharpness while maintaining communication efficiency*?

5.1.1. Challenges of Server-side SAM

We address this question by applying SAM on the server side, directly optimizing for global sharpness and eliminating the need to align local sharpness on the clients. The global model has to be updated as $\boldsymbol{w}^{t+1} \leftarrow$

Table 2. Overview of FL methods using SAM. Differently from previous works, FEDGLOSS uses SAM as server optimizer and allows any local optimizer.

Method	SERVEROPT	CLIENTOPT	Global Flatness	Communication Cost	Local Computation Cost
FEDSAM [4, 45]	SGD	SAM	✗	1×	2×
FEDDYN [1] + SAM	SGD	SAM	✗	1×	2×
FEDSPEED [54]	SGD	Similar to SAM	✗	1×	2×
FEDGAMMA [7]	SGD	SAM	✓	2×	2×
FEDSMOO [53]	SGD	SAM	✓	2×	2×
FEDGLOSS	**SAM**	**Any optimizer**	✓	1×	1× or 2×

$\boldsymbol{w}^t - \eta_s \nabla_{\boldsymbol{w}} \mathcal{F}(\boldsymbol{w})|_{\boldsymbol{w}^t + \hat{\boldsymbol{\epsilon}}^t(\boldsymbol{w})}$, where $\hat{\boldsymbol{\epsilon}}^t$ is the global perturbation at each round t. However, a key challenge arises: the computation of both $\hat{\boldsymbol{\epsilon}}^t$ and the sharpness-aware gradient necessitates two transmissions with the clients, making its direct application in server-side FL non-trivial. A straightforward solution is to emulate SAM's double computation step through two communication exchanges $\forall t \in [T]$.

- **Step 1**: the server sends the global model $\boldsymbol{w}^t$ to a subset $\mathcal{C}^t$ of clients, which update it using their local data. With the resulting pseudo-gradient $\Delta^t_{\boldsymbol{w}}$, $\hat{\boldsymbol{\epsilon}}^t(\boldsymbol{w}) = \rho(\Delta^t_{\boldsymbol{w}}/\|\Delta^t_{\boldsymbol{w}}\|)$ and the perturbed model $\tilde{\boldsymbol{w}}^t = \boldsymbol{w}^t + \hat{\boldsymbol{\epsilon}}^t(\boldsymbol{w})$.
- **Step 2**: the server transmits $\tilde{\boldsymbol{w}}^t$ to the *same* $\mathcal{C}^t$, which compute their update $\tilde{\boldsymbol{w}}^t_k \ \forall k$. The resulting global pseudo-gradient $\tilde{\Delta}^t_{\boldsymbol{w}} \triangleq \sum_{k\in\mathcal{C}^t} {}^{N_k}\!/_N(\tilde{\boldsymbol{w}}^t - \tilde{\boldsymbol{w}}^t_k)$ is an estimate of $\nabla_{\boldsymbol{w}} \mathcal{F}(\boldsymbol{w})|_{\boldsymbol{w}^t + \hat{\boldsymbol{\epsilon}}^t(\boldsymbol{w})}$.

This two-step approach, referred to as NAIVEFEDGLOSS, is conceptually simple but suffers from communication *in*efficiency, doubling the communication cost w.r.t. FedAvg, while requiring the same set of clients $\mathcal{C}^t$ to remain active for two consecutive exchanges. This may be unrealistic in real-world settings often characterized by network failures. These limitations highlight the need for an efficient alternative that accounts for practical real-world FL factors.

5.2. FedGloSS

To overcome the challenges posed by NAIVEFEDGLOSS, following [42], FEDGLOSS estimates $\hat{\boldsymbol{\epsilon}}^t$ using the perturbed global pseudo-gradient from the previous round $\tilde{\Delta}^{t-1}_{\boldsymbol{w}}$ at each round t. This approach leverages available information *without incurring extra communications* and avoids unnecessary computations. Intuitively, the use of the previous pseudo-gradient to minimize the sharpness allows FEDGLOSS to access information on the *global* loss landscape geometry, thus guiding the *global* optimization towards flatter minima. From Eqs. (3) and (5), FEDGLOSS updates the global model $\boldsymbol{w}^t$ as

$$\text{① } \tilde{\boldsymbol{\epsilon}}^t(\boldsymbol{w}) \triangleq \rho \frac{\tilde{\Delta}^{t-1}_{\boldsymbol{w}}}{\|\tilde{\Delta}^{t-1}_{\boldsymbol{w}}\|} \quad \text{② } \tilde{\boldsymbol{w}}^t \leftarrow \boldsymbol{w}^t + \tilde{\boldsymbol{\epsilon}}^t(\boldsymbol{w})$$

$$\text{③ Obtain } \tilde{\boldsymbol{w}}^t_k \text{ from clients and } \tilde{\Delta}^t_{\boldsymbol{w}} = \sum_{k\in\mathcal{C}^t} \frac{N_k}{N}(\tilde{\boldsymbol{w}}^t - \tilde{\boldsymbol{w}}^t_k)$$

$$\text{④ } \boldsymbol{w}^{t+1} \leftarrow \boldsymbol{w}^t - \text{FEDGLOSS}(\boldsymbol{w}^t, \tilde{\Delta}^t_{\boldsymbol{w}}, \eta_s) = \boldsymbol{w}^t - \eta_s \tilde{\Delta}^t_{\boldsymbol{w}},$$

where with a slight abuse of notation SERVEROPT from Eq. (3) is substituted with the server-side strategy proposed by FEDGLOSS. The notation follows the colors of Fig. 3, which depicts our approach. Notably, as summarized in Tab. 2, FEDGLOSS enables SAM on the server side while allowing any CLIENTOPT for local training, with computational costs varying based on the chosen optimizer. This differs from previous methods constrained to the more computationally expensive SAM. In addition, differently from FEDSMOO, FEDGLOSS maintains FEDAVG's communication complexity while optimizing for global flatness.

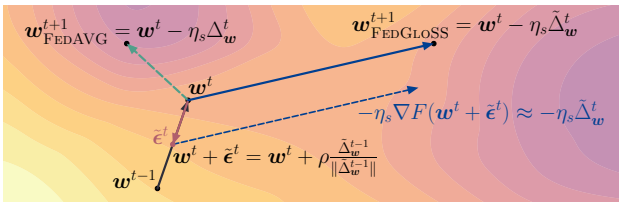


Figure 3. Illustration of FEDGLOSS. The model $\boldsymbol{w}^t$ is perturbed using $\tilde{\Delta}^{t-1}_{\boldsymbol{w}}$. The sharpness-aware direction (*dashed*) is used to compute $\boldsymbol{w}^{t+1}$ (*solid*), which lands in a flat region. Compared to FEDAVG.

5.2.1. Promoting Global Consistency with ADMM

The difference in using the approximation $\tilde{\boldsymbol{\epsilon}}^t$ (FEDGLOSS) and the true $\hat{\boldsymbol{\epsilon}}^t$ (NAIVEFEDGLOSS) is

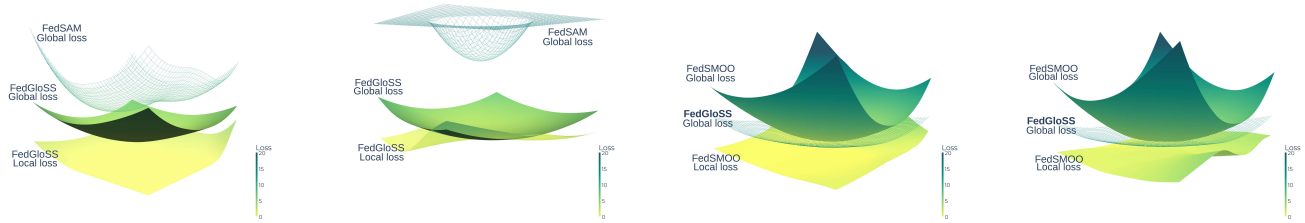
$$\delta^t_\epsilon \triangleq \|\tilde{\boldsymbol{\epsilon}}^t(\boldsymbol{w}) - \hat{\boldsymbol{\epsilon}}^t(\boldsymbol{w})\| = \rho \left\| \frac{\tilde{\Delta}^{t-1}_{\boldsymbol{w}}}{\|\tilde{\Delta}^{t-1}_{\boldsymbol{w}}\|} - \frac{\Delta^t_{\boldsymbol{w}}}{\|\Delta^t_{\boldsymbol{w}}\|} \right\|, \quad (6)$$

where $\tilde{\Delta}^{t-1}_{\boldsymbol{w}}$ is computed using the updates of the clients in $\mathcal{C}^{t-1}$ and $\tilde{\Delta}^t_{\boldsymbol{w}}$ with $\mathcal{C}^t$. Eq. (6) suggests δ^t_ϵ is minimized when $\tilde{\Delta}^{t-1}_{\boldsymbol{w}}$ and $\tilde{\Delta}^t_{\boldsymbol{w}}$ are aligned, which occurs when clients' updates are directionally consistent. However, in real-world heterogeneous FL, *i*) to due clients' unavailability, only a subset of them participates in training at each round, with $\mathcal{C}^t$ likely differing from $\mathcal{C}^{t-1}$, and *ii*) clients hold different data distributions, *i.e.*, local optimization paths likely converge towards different local minima, leading to unstable global updates [26]. As a consequence, $\delta^t_\epsilon \not\to 0$ necessarily.

To align local and global objectives - guiding client and server updates in the same direction and minimizing Eq. (6) - FEDGLOSS leverages the Alternating Direction Method of Multipliers (ADMM) [3] on $\boldsymbol{w}^t$ [1, 53, 54]. While alternative approaches could be used, they either lack full immunity to data heterogeneity or have shown poor performance on realistic scenarios (*e.g.*, variance reduction [7, 26]). In contrast, ADMM has been proved to converge under arbitrary heterogeneity [1] and can thus be leveraged as a base algorithm for FEDGLOSS, as shown in Alg. 1 in App. A. ADMM makes use of the augmented Lagrangian function $\mathcal{L}(\boldsymbol{w}, \boldsymbol{W}, \sigma) = \sum_{k\in\mathcal{C}} L(\boldsymbol{w}, \boldsymbol{w}_k, \sigma_k)$ where $\boldsymbol{W} = \{\boldsymbol{w}_1, \cdots, \boldsymbol{w}_C\}$ and σ is the Lagrangian multiplier. The problem solved by $\mathcal{L}$ is

$$\frac{1}{C}\sum_{k\in\mathcal{C}}(f_k + \sigma_k^\top(\boldsymbol{w}^t - \boldsymbol{w}^t_k) + \frac{1}{2\beta}\|\boldsymbol{w}^t - \boldsymbol{w}^t_k\|^2) \ s.t. \ \boldsymbol{w} = \boldsymbol{w}_k \quad (7)$$

with $\beta > 0$ being an hyperparameter. Eq. (7) is split into C sub-problems of the form $\boldsymbol{w}_{k,E} = \text{argmin}_{\boldsymbol{w}_k}\{f_k - \sigma_k^\top(\boldsymbol{w}^t - \boldsymbol{w}_k) + \frac{1}{2\beta}\|\boldsymbol{w}^t - \boldsymbol{w}^t_k\|^2\}$. The local dual variable is updated as $\sigma_k \leftarrow \sigma_k - \frac{1}{\beta}(\boldsymbol{w}^t_{k,E} - \boldsymbol{w}^t_{k,0})$. The global one σ is updated by adding the averaged $\boldsymbol{w}_k - \boldsymbol{w}^t \ \forall k \in \mathcal{C}$. We note that ADMM introduces a key limitation of our approach, namely reliance on stateful clients. Fig. 5 confirms



(a) Local model on class `sea` w/ FEDGLOSS

(b) Local model on class `snail` w/ FEDGLOSS

(c) Local model on class `sea` w/ FEDSMOO

(d) Local model on class `snail` w/ FEDSMOO

Figure 4. **Global *vs.* local perspective of FEDGLOSS and FEDSMOO.** Loss landscapes of clients models trained on one `class`, tested on the local ("*Local loss*") or global dataset ("*Global loss*"). CIFAR100 $\alpha = 0$ with SAM as local optimizer @ $t = 20k$, CNN. **(a)-(b):** Models trained with FEDGLOSS. Global loss of FEDSAM's local model (*net*) as reference. **(c)-(d)**: Models trained with FEDSMOO. Global loss of FEDGLOSS' local model (*net*) as reference. **FEDGLOSS achieves better consistency w.r.t. FEDSMOO.**

the directional consistency of local and global updates enforced by ADMM reduces δ_ϵ^t (Eq. (6)), *i.e.*, the difference between the true and approximated perturbation. The gap between the directions of $\tilde{\Delta}_{\boldsymbol{w}}^{t-1}$ and $\tilde{\Delta}_{\boldsymbol{w}}^{t}$ remains constant after an initial phase, suggesting the most challenging loss landscape direction is largely stable over time.

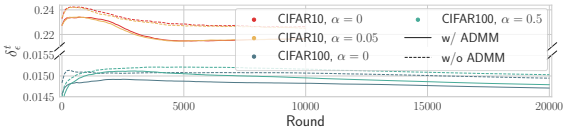


Figure 5. Trend of the difference δ_ϵ^t (Eq. (6)), which decreases as ADMM is used and over training rounds. CIFAR datasets, CNN.

6. Experiments

6.1. Experimental Setting

App. C details implementation and hyperparameter settings.

Federated datasets. We leverage established FL benchmarks [6, 19, 20]. *Small-scale image classification:* following [4, 20], the federated versions of CIFAR10 (10 classes) and CIFAR100 (100 classes) [29] split the respective $50k$ training images in 100 clients with 500 images each. The data distribution is controlled by Dirichlet's parameter $\alpha \in \{0, 0.05, 1, 5, 10\}$ for CIFAR10 and $\{0, 0.5\}$ for CIFAR100 [19]. Lower α signifies increased heterogeneity, with $\alpha = 0$ being the most challenging scenario (each client holds samples from one class). *Large-scale image classification:* LANDMARKS-USER-160K ($2,028$ classes) [20] is the federated Google Landmarks v2 [58] with $164,172$ pictures of worldwide locations, split among $1,262$ realistic clients.

Models. The effectiveness of FEDGLOSS is shown using multiple model architectures. As in [4, 20], we use a Convolutional Neural Network (CNN) similar to LeNet5 [30] on both CIFAR10 ($T = 10k$) and CIFAR100 ($T = 20k$). Experiments with ResNet18 [16] run for $10k$ rounds. For LANDMARKS-USER-160K, we train MobileNetv2 [20, 50] ($T = 1.3k$), considering the limited resources at the edge.

Baselines. To study real-world settings with varying participation, a small fraction of clients is sampled at each round, with participation rate set to 5% with the CNN and 10% with ResNet18 on both CIFARs, and to 50 clients per round in LANDMARKS-USER-160K ($\approx 4\%$). FEDGLOSS is compatible with any local optimizer (Sec. 5). We choose SGD and SAM to comply with previous works and compare it with state-of-the-art (SOTA) methods for statistical heterogeneity in FL, distinguishing the results by optimizer type to highlight performance differences. SGD-based approaches are FedAvg [39], FedProx [35], FedDyn [1] and Scaffold [26], while use SAM FedSAM [4, 45], FedDyn + SAM, FedSpeed [54], FedGamma [7] and FedSmoo [53].

6.2. Achieving Local-Global Sharpness Consistency

To assess the effectiveness of FEDGLOSS in promoting consistency between local and global loss landscapes, Fig. 4 replicates the analysis previously conducted on FEDSAM (Fig. 2). The behavior of local models is shown from both local ("*Local loss*") and global perspectives ("*Global loss*"). App. B.1 offers visualizations for the remaining clients. Compared to FEDSAM, the gap between local and global loss landscapes in FEDGLOSS is significantly smaller, and both global and local loss surfaces are found in *flat and low-loss regions* (Figs. 4a and 4b). This suggests our method effectively promotes convergence toward aligned low-loss flat regions, minimizing the discrepancy between local and global geometries. This results in a global model residing in a flat minimum in the global landscape (Figs. 6a and 6c). Figs. 4c and 4d instead compare FEDGLOSS with the best-performing SOTA FEDSMOO, where the position in the global landscape of FEDGLOSS' local models is added for reference. While FEDSMOO improves consistency between local and global sharpness compared to FEDSAM, it falls short of FEDGLOSS in reaching a flatter global minimum.

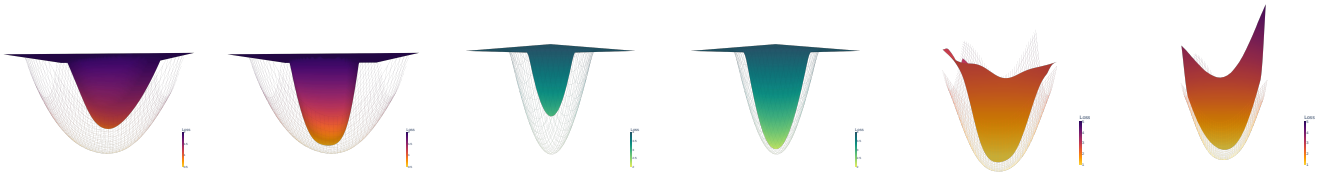
Tab. 1 confirms these claims. By combining ADMM for consistency and server-side SAM for global flatness, FEDGLOSS prioritizes achieving a flatter *global* region during training, as proven by the lowest global maximum eigenvalue $\lambda_{1,g}$ and larger $\lambda_{1,l}$, across all clients and methods.

6.3. Benchmarking FedGloSS against SOTA

This section compares FEDGLOSS with SOTA methods on vision tasks in heterogeneous FL. App. B.4 presents results for $\alpha \in \{1, 5, 10\}$ on CIFAR10 and homogeneous settings.

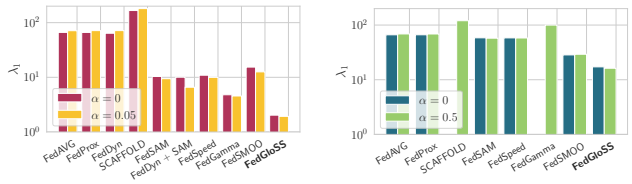
6.3.1. FedGloSS on Standard Federated Benchmarks

Tab. 3 presents results on CIFAR100 and CIFAR10 with varying levels of heterogeneity on the CNN model. Several observations highlight the advantages of FEDGLOSS. FEDGLOSS achieves the best results among both SGD and SAM-based approaches while maintaining communication



(a) C10 $\alpha = 0$ CNN FEDGLOSS *vs.* FEDSAM (b) C10 $\alpha = 0$ CNN FEDGLOSS *vs.* FEDSMOO (c) C100 $\alpha = 0$ CNN FEDGLOSS *vs.* FEDSAM (d) C100 $\alpha = 0$ CNN FEDGLOSS *vs.* FEDSMOO (e) C10 $\alpha = 0.05$ ResNet18 FEDGLOSS *vs.* FEDSAM (f) C10 $\alpha = 0.05$ ResNet18 FEDGLOSS *vs.* FEDSMOO

Figure 6. **Loss landscapes of models trained with FEDGLOSS (*net*) *vs.* FEDSAM and FEDSMOO (*solid*)** on CIFAR10/100. **(a) - (c) - (e):** The flatter regions reached by FEDGLOSS w.r.t. FEDSAM prove the effectiveness of optimizing for global flatness. **(b) - (d) - (f):** FEDGLOSS achieves flatter minima and lower loss values w.r.t. FEDSMOO.



(a) CIFAR10 (b) CIFAR100

Figure 7. **Maximum Hessian eigenvalues** (λ_1), CNN. Values shown only if algorithm converged. **FEDGLOSS reaches the flattest global minima**.

Table 3. **FEDGLOSS *vs.* the state of the art** on CIFAR datasets, distinguished by local optimizer, SGD (*top*) and SAM (*bottom*), in terms of communication cost and accuracy (%). Best results in **bold**. Model: CNN.

	Method	Comm. Cost	CIFAR10 $\alpha = 0$	CIFAR10 $\alpha = 0.05$	CIFAR100 $\alpha = 0$	CIFAR100 $\alpha = 0.5$
Client SGD	FEDAVG	1×	59.9±0.4	65.7±1.0	28.6±0.7	38.5±0.5
	FEDPROX	1×	59.8±0.5	65.6±1.0	28.8±0.7	38.7±0.4
	FEDDYN	1×	65.5±0.3	70.1±1.2	✗	✗
	SCAFFOLD	2×	25.1±3.7	54.0±2.6	✗	30.0±1.1
	FEDGLOSS	1×	**69.5±0.4**	**75.5±0.3**	**42.5±0.6**	**47.9±0.5**
Client SAM	FEDSAM	1×	70.2±0.9	71.5±1.08	28.7±0.5	39.6±0.5
	FEDDYN	1×	79.3±3.1	81.5±0.6	✗	✗
	FEDSPEED	1×	70.9±0.4	72.3±1.1	28.9±0.5	39.7±0.5
	FEDGAMMA	2×	58.9±1.8	61.9±1.8	✗	29.4±1.4
	FEDSMOO	2×	81.3±0.5	82.8±0.6	47.8±0.5	51.7±0.46
	FEDGLOSS	1×	**83.9±0.4**	**84.4±0.5**	**50.6±0.6**	**53.4±0.5**

efficiency. FEDGLOSS with local SAM consistently outperforms the best-performing SOTA FEDSMOO by ≈ 2.5 percentage points in accuracy across all configurations *with half the communication cost*. Our method reaches the flattest global minima (*e.g.*, $\lambda_1^{\text{FEDGLOSS}} = 2.03$ *vs.* $\lambda_1^{\text{FEDSMOO}} = 15.37$ on CIFAR10 $\alpha = 0$), as shown in Figs. 6 and 7, achieving the best overall performance. FEDGLOSS with local SGD overcomes by ≈ 4 percentage points *all* SGD-based approaches. FEDDYN suffers from parameter explosion in highly heterogeneous settings [56], failing to converge on CIFAR100. Differently, FEDGLOSS successfully employs ADMM to align global and local solutions, with the best results under extreme heterogeneity. Studies showed SCAFFOLD performs poorly in complex heterogeneous environments [4, 33], resulting in its inability to converge on CIFAR100 alongside FEDGAMMA. Tab. 4 confirms FEDGLOSS' effectiveness, consistently outperforming SOTA methods with the more complex ResNet18 architecture, with ≈ 8 points higher accuracy w.r.t. FEDAVG with both SGD and SAM, and +5 w.r.t. FEDSMOO, with the flattest solutions (Figs. 6e and 6f).

6.3.2. FedGloSS on Real-World Large-Scale Datasets

To further highlight FEDGLOSS's effectiveness, we evaluate it on *large-scale image classification* using the challenging LANDMARKS-USER-160K dataset. Tab. 5 compares FEDGLOSS with local SAM against the best-performing

Table 4. **ResNet18** on CIFAR100 $\alpha = 0.5$ and CIFAR10 $\alpha = 0.05$.

	Method	Comm. cost	C100 Acc.	C10 Acc.
Client SGD	FEDAVG	1×	37.4±0.2	72.6±0.1
	FEDPROX	1×	37.6±0.1	72.2±0.2
	FEDDYN	1×	38.8±0.6	70.2±0.6
	SCAFFOLD	2×	38.6±0.1	70.8±0.6
	FEDGLOSS	1×	**46.7±0.6**	**79.1±0.5**
Client SAM	FEDSAM	1×	38.5±0.1	72.8±0.1
	FEDDYN	1×	39.6±0.8	72.6±0.2
	FEDSPEED	1×	38.7±0.6	72.6±0.1
	FEDGAMMA	2×	38.8±0.3	72.2±0.1
	FEDSMOO	2×	44.8±0.5	75.3±0.6
	FEDGLOSS	1×	**47.2±0.2**	**80.0±0.3**

Table 5. **MobileNetv2** on LANDMARKS-USER-160K.

Method	Comm. cost	Accuracy
FEDAVG	1×	56.3±0.2
FEDPROX	1×	55.0±0.2
FEDDYN	1×	55.2±0.6
SCAFFOLD	2×	✗
FEDSAM	1×	56.7±0.1
FEDDYN + SAM	1×	56.0±1.3
FEDGAMMA	2×	✗
FEDSMOO	2×	59.5±0.1
FEDGLOSS	1×	**59.7±1.2**

baselines. FEDGLOSS is among the few methods, alongside FEDSAM and FEDSMOO, outperforming FEDAVG. Similarly to the CIFAR100 results (Sec. 6.3.1), both SCAFFOLD and FEDGAMMA fail to converge. Importantly, FEDGLOSS achieves the best overall performance (+3.4% w.r.t. FEDAVG) with reduced communication overhead.

6.3.3. ADMM and SAM Interaction in FedGloSS

ADMM-based methods are often prone to parameter explosion in highly heterogeneous FL settings with many clients [56]. This occurs as multiple gradients accumulate in the global dual variable σ (Sec. 5), causing the parameter norms to grow uncontrollably. However, empirical results indicate this issue is mitigated with SAM (*e.g.*, see FEDDYN *vs.* FEDGLOSS in Tab. 3). We attribute this to SAM 's nature: by targeting flat minima, it promotes smaller gradient steps and minimal weight updates, resulting in a more stable algorithm. Fig. 8 confirms our hypothesis by showing SAM's stability effectively lowers parameter norms and the consequent risk of explosion, particularly when SAM is applied directly to the global model, as in FEDGLOSS.

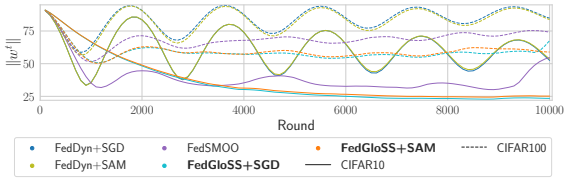


Figure 8. **Trend of model parameters norm**, $\| \boldsymbol{w}^t \|_2$, on SAM-based methods with ResNet18 on CIFAR datasets. **SAM reduces the norm and the risk of parameters explosion, successfully enabling ADMM in heterogeneous FL**.

6.3.4. Communication Efficiency with FedGloSS

Communication cost is the main bottleneck in FL [32], making its optimization a relevant challenge. As already previously highlighted, FEDGLOSS considers communication efficiency its primacy concern. Defined B the number of bits exchanged by FEDAVG in T training rounds, Tab. 6 studies FEDGLOSS's communication cost against the SOTA baselines in terms of rounds necessary to reach FEDAVG's performance and quantity of exchanged bits.

Table 6. **Communication costs** comparison w.r.t. FEDAVG. "-" for not reached accuracy, "✗" for non-convergence. GLDV2 is LANDMARKS-USER-160K.

	Method	CNN				ResNet18				MobileNetv2	
		CIFAR10 $\alpha=0$		CIFAR100 $\alpha=0$		CIFAR10 $\alpha=0.05$		CIFAR100 $\alpha=0.5$		GLDV2	
		Rounds	*Cost*	*Rounds*	*Cost*	*Rounds*	*Cost*	*Rounds*	*Cost*	*Rounds*	*Cost*
Client SGD	FEDAVG	$10k$	$1B$	$20k$	$1B$	$10k$	$1B$	$10k$	$1B$	$1.3k$	$1B$
	FEDPROX	$7.6k$	$0.8B$	$18.7k$	$0.9B$	$8.8k$	$0.9B$	$8.3k$	$0.8B$	-	-
	FEDDYN	$2k$	$\mathbf{0.2B}$		✗	-	-	$3.5k$	$0.4B$	-	-
	SCAFFOLD	-	-	-	-	-	-	$8.9k$	$1.8B$		✗
	FEDGLOSS	$3.4k$	$0.3B$	$5k$	$\mathbf{0.3B}$	$2.4k$	$\mathbf{0.2B}$	$1.9k$	$\mathbf{0.2B}$	$1.3k$	$1B$
Client SAM	FEDSAM	$6.3k$	$0.6B$	$18.3k$	$0.9B$	$9.2k$	$0.9B$	$7.8k$	$0.8B$	$1.3k$	$1B$
	FEDDYN	$3k$	$0.3B$		✗	$4.1k$	$0.4B$	$3.5k$	$0.4B$	-	-
	FEDSPEED	$6.3k$	$0.6B$	$18.3k$	0.9B	$8.3k$	$0.8B$	$8.3k$	$0.8B$	$1.3k$	$1B$
	FEDGAMMA	-	-	-	-	$9.3k$	$1.9B$	$8.1k$	$1.6B$		✗
	FEDSMOO	$1.9k$	$0.4B$	$4.5k$	$0.5B$	$2.4k$	$0.5B$	$2.3k$	$0.5B$	200	$0.4B$
	FEDGLOSS	$2.2k$	$\mathbf{0.2B}$	$6.3k$	$\mathbf{0.3B}$	$2.4k$	$\mathbf{0.2B}$	$1.9k$	$\mathbf{0.2B}$	200	$\mathbf{0.2B}$

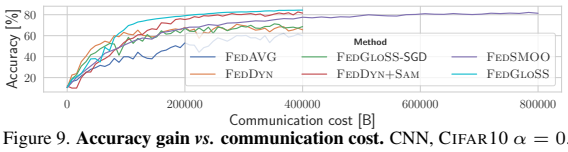


Figure 9. **Accuracy gain *vs.* communication cost.** CNN, CIFAR10 $\alpha = 0$.

The ADMM-based methods are usually faster, with FEDGLOSS being the fastest with ResNet18 and MobileNetv2. While FEDSMOO is faster when using the CNN model, the transmitted bits double due to its increased communication cost, making FEDGLOSS the most efficient method in all cases. Analyses on left-out settings in App. B.5. Fig. 9 further shows the *total* communication cost of the FL algorithms (*# model exchanges per round* $\times|\mathcal{C}^t| \times T$). The doubled cost of FEDSMOO is clear, while FEDGLOSS achieves nearly double FEDAVG's accuracy at the same cost.

6.4. Ablation Studies

6.4.1. Communication-efficient Sharpness

This section evaluates using the pseudo-gradient from the previous round $\tilde{\Delta}_{\boldsymbol{w}}^{t-1}$ (Eq. (6)) to estimate sharpness. FEDGLOSS leverages past gradients as a reliable indication on the global loss landscape and aligns global and local paths via ADMM for consistent trajectories across rounds.

Tab. 7 compares FEDGLOSS with its baseline, NAIVEFEDGLOSS (Sec. 5), which computes the exact perturbation $\hat{\boldsymbol{\epsilon}}^t$ at the expense of doubled communication costs. FEDGLOSS matches NAIVEFEDGLOSS in accuracy while maintaining communication efficiency, with minimal or negligible gap in performance, consistent with similar sharpness (λ_1). To fairly assess communication costs, Tab. 7 also reports FEDGLOSS' final accuracy *vs.* NAIVEFEDGLOSS' performance at 50% training progress, showing FEDGLOSS' higher accuracy given the same number of exchanges. Overall, given B bits transmitted by FEDGLOSS, the cost of NAIVEFEDGLOSS is $1.96B$ on C10 $\alpha = 0$, $2B$ for $\alpha = 0.05$, $1.94B$ on C100 $\alpha = 0$ and $1.97B$ for $\alpha = 0.5$. Thus, FEDGLOSS reduces communication costs by up to 50%, with no trade-off in model performance. If NAIVEFEDGLOSS were preferred to maintain exact gradients, it would still achieve the *best results* with costs *lower or comparable* to FEDSMOO. In addition, our strategy in centralized settings lowers the performance w.r.t. SAM, thus reducing our centralized upper bound w.r.t. NAIVEFEDGLOSS. At equal performance, FEDGLOSS narrows the gap to the upper bound: -2.4% on CIFAR10 with $\alpha = 0$ and -1.9% with $\alpha = 0.05$ *vs.* respectively -3.2% and -2.7% of NAIVEFEDGLOSS w.r.t. SAM. In CIFAR100 instead, -7% on $\alpha = 0$ and -4.2% on $\alpha = 0.5$ of FEDGLOSS *vs.* -8.1% and -5.2% of its baseline. Aiming to reduce communication bottlenecks and improve performance, these results validate choosing FEDGLOSS over NAIVEFEDGLOSS. Further analyses in App. B.5.

Table 7. **FEDGLOSS *vs.* NAIVEFEDGLOSS** in terms of communication cost, accuracy (50% and 100% of training) and maximum Hessian eigenvalue λ_1. SAM as CLIENTOPT. CIFAR datasets with $\alpha = 0$ (*top*) and $\alpha = 0.05/0.5$ (*bottom*). $\widetilde{\text{SAM}}$ is SAM with the sharpness approximation of FEDGLOSS, using the previous gradient.

Method	Comm. Cost	CIFAR10 Acc@50%	CIFAR10 Acc@100%	CIFAR10 λ_1 (↓)	CIFAR100 Acc@50%	CIFAR100 Acc@100%	CIFAR100 λ_1 (↓)
NAIVEFEDGLOSS	2×	$77.6_{\pm 0.3}$	$\mathbf{83.9}_{\pm 0.2}$	$2.78_{\pm 0.13}$	$\mathbf{42.6}_{\pm 0.8}$	$\mathbf{50.8}_{\pm 0.1}$	$\mathbf{16.93}_{\pm 0.27}$
FEDGLOSS	1×	$\mathbf{78.9}_{\pm 0.5}$	$\mathbf{83.9}_{\pm 0.4}$	$\mathbf{2.03}_{\pm 0.05}$	$39.5_{\pm 0.9}$	$50.6_{\pm 0.6}$	$17.18_{\pm 0.97}$
NAIVEFEDGLOSS	2×	$78.7_{\pm 0.1}$	$\mathbf{84.4}_{\pm 0.2}$	$2.75_{\pm 0.09}$	$\mathbf{49.4}_{\pm 0.5}$	$\mathbf{53.7}_{\pm 0.3}$	$\mathbf{15.84}_{\pm 0.52}$
FEDGLOSS	1×	$\mathbf{79.7}_{\pm 0.4}$	$\mathbf{84.4}_{\pm 0.5}$	$\mathbf{1.93}_{\pm 0.03}$	$47.2_{\pm 1.1}$	$53.4_{\pm 0.5}$	$16.22_{\pm 0.35}$
Centralized		87.1 SAM	86.3 $\widetilde{\text{SAM}}$		58.4 SAM	57.6 $\widetilde{\text{SAM}}$	

6.4.2. The Role of Global Consistency and Flatness

Tab. 8 isolates the impact of global consistency and global sharpness minimization in FEDGLOSS. We recall FEDAVG with client-side SAM is FEDSAM and using ADMM only for aligning local and global convergence points is FEDDYN. Both components significantly impact performance, with their combination leading FEDGLOSS to the best overall results. FEDGLOSS is not prone to parameter explosion, achieving the best results even where FEDDYN fails to converge (✗). The flatness of FEDGLOSS' solutions w.r.t. FEDSAM in Fig. 6 confirms the efficacy of its strategy.

Table 8. Efficacy of global sharpness minimization in FEDGLOSS: ADMM for global consistency and server-side SAM for global sharpness minimization lead to the best performance. CIFARS, CNN with $\alpha = 0$ and ResNet18 with $\alpha \in \{0.05, 0.5\}$.

CLIENT OPT	Method	Global Consistency	Global Flatness	CNN CIFAR10	CNN CIFAR100	ResNet18 CIFAR10	ResNet18 CIFAR100
SAM	FEDSAM	✗	✗	70.2 ± 0.9	28.7 ± 0.5	72.8 ± 0.1	38.5 ± 0.1
	FEDDYN	✓	✗	79.3 ± 3.1	✗	72.6 ± 0.2	39.6 ± 0.8
	FEDGLOSS	✓	✓	$\mathbf{83.9\pm0.4}$	$\mathbf{50.6\pm0.6}$	$\mathbf{80.0\pm0.3}$	$\mathbf{47.2\pm0.2}$
SGD	FEDAVG	✗	✗	59.9 ± 0.4	28.6 ± 0.7	72.6 ± 0.1	37.4 ± 0.2
	FEDDYN	✓	✗	65.5 ± 0.3	✗	70.2 ± 0.6	38.8 ± 0.6
	FEDGLOSS	✓	✓	$\mathbf{69.5\pm0.4}$	$\mathbf{42.5\pm0.6}$	$\mathbf{79.1\pm0.5}$	$\mathbf{46.7\pm0.6}$

7. Conclusion

This work tackled the challenge of limited generalization in heterogeneous Federated Learning (FL), prioritizing communication efficiency for real-world use. Building on research linking poor generalization to sharp minima in the loss landscape, we showed data heterogeneity worsens discrepancies between local and global loss surfaces, a problem not resolved by methods focusing only on local sharpness. To address this, our Federated Global Server-side Sharpness (FedGloSS) finds flat minima in the *global* loss landscape with server-side Sharpness-Aware Minimization and achieves communication efficiency by approximating SAM's sharpness through past global pseudo-gradients, distinguishing it from prior approaches. This work revealed SAM prevents ADMM-related parameter explosion by guiding optimization along flat directions, enabling stable updates in heterogeneous FL. Extensive evaluations showed FedGloSS outperforms SOTA methods in accuracy, flatness and communication efficiency.

Acknowledgments. This study was carried out within the FAIR - Future Artificial Intelligence Research and received funding from the European Union Next-GenerationEU (PIANO NAZIONALE DI RIPRESA E RESILIENZA (PNRR) – MISSIONE 4 COMPONENTE 2, INVESTIMENTO 1.3 – D.D. 1555 11/10/2022, PE00000013). This manuscript reflects only the authors' views and opinions, neither the European Union nor the European Commission can be considered responsible for them. We acknowledge the CINECA award under the ISCRA initiative for the availability of high-performance computing resources and support.

References

[1] Durmus Alp Emre Acar, Yue Zhao, Ramon Matas Navarro, Matthew Mattina, Paul N Whatmough, and Venkatesh Saligrama. Federated learning based on dynamic regularization. *ICLR*, 2021. 1, 2, 3, 5, 6, 16, 18, 19

[2] Rodolfo Stoffel Antunes, Cristiano André da Costa, Arne Küderle, Imrana Abdullahi Yari, and Björn Eskofier. Federated learning for healthcare: Systematic review and architecture proposal. *ACM Transactions on Intelligent Systems and Technology (TIST)*, 13(4):1–23, 2022. 1

[3] Stephen Boyd, Neal Parikh, Eric Chu, Borja Peleato, Jonathan Eckstein, et al. Distributed optimization and statistical learning via the alternating direction method of multipliers. *Foundations and Trends® in Machine learning*, 3 (1):1–122, 2011. 2, 5

[4] Debora Caldarola, Barbara Caputo, and Marco Ciccone. Improving generalization in federated learning by seeking flat minima. In *European Conference on Computer Vision*, pages 654–672. Springer, 2022. 1, 2, 3, 4, 5, 6, 7, 16, 18, 19, 20

[5] Debora Caldarola, Barbara Caputo, and Marco Ciccone. Window-based model averaging improves generalization in heterogeneous federated learning. In *Proceedings of the IEEE/CVF International Conference on Computer Vision*, pages 2263–2271, 2023. 3, 19

[6] Sebastian Caldas, Sai Meher Karthik Duddu, Peter Wu, Tian Li, Jakub Konečnỳ, H Brendan McMahan, Virginia Smith, and Ameet Talwalkar. Leaf: A benchmark for federated settings. *Workshop on Data Privacy and Confidentiality*, 2019. 6

[7] Rong Dai, Xun Yang, Yan Sun, Li Shen, Xinmei Tian, Meng Wang, and Yongdong Zhang. Fedgamma: Federated learning with global sharpness-aware minimization. *IEEE Transactions on Neural Networks and Learning Systems*, 2023. 1, 2, 5, 6

[8] Jia Deng, Wei Dong, Richard Socher, Li-Jia Li, Kai Li, and Li Fei-Fei. Imagenet: A large-scale hierarchical image database. In *2009 IEEE conference on computer vision and pattern recognition*, pages 248–255. Ieee, 2009. 19

[9] Jiawei Du, Hanshu Yan, Jiashi Feng, Joey Tianyi Zhou, Liangli Zhen, Rick Siow Mong Goh, and Vincent YF Tan. Efficient sharpness-aware minimization for improved training of neural networks. *ICLR*, 2022. 3

[10] Jiawei Du, Daquan Zhou, Jiashi Feng, Vincent Tan, and Joey Tianyi Zhou. Sharpness-aware training for free. *Advances in Neural Information Processing Systems*, 35: 23439–23451, 2022. 3

[11] Lidia Fantauzzo, Eros Fanì, Debora Caldarola, Antonio Tavera, Fabio Cermelli, Marco Ciccone, and Barbara Caputo. Feddrive: Generalizing federated learning to semantic segmentation in autonomous driving. In *2022 IEEE/RSJ International Conference on Intelligent Robots and Systems (IROS)*, pages 11504–11511. IEEE, 2022. 1, 2

[12] Pierre Foret, Ariel Kleiner, Hossein Mobahi, and Behnam Neyshabur. Sharpness-aware minimization for efficiently improving generalization. *Int. Conf. Machine Learn.*, 2021. 1, 2, 3, 20

[13] Liang Gao, Huazhu Fu, Li Li, Yingwen Chen, Ming Xu, and Cheng-Zhong Xu. Feddc: Federated learning with non-iid data via local drift decoupling and correction. In *Proceedings of the IEEE/CVF conference on computer vision and pattern recognition*, pages 10112–10121, 2022. 3

[14] Timur Garipov, Pavel Izmailov, Dmitrii Podoprikhin, Dmitry P Vetrov, and Andrew G Wilson. Loss surfaces, mode connectivity, and fast ensembling of dnns. *Advances in neural information processing systems*, 31, 2018. 20

[15] Noah Golmant, Zhewei Yao, Amir Gholami, Michael Mahoney, and Joseph Gonzalez. pytorch-hessian-eigenthings: efficient pytorch hessian eigendecomposition, 2018. 20

[16] Kaiming He, Xiangyu Zhang, Shaoqing Ren, and Jian Sun. Deep residual learning for image recognition. corr abs/1512.03385 (2015), 2015. 6, 19

[17] Sepp Hochreiter and Jürgen Schmidhuber. Flat minima. *Neural computation*, 9(1):1–42, 1997. 1, 2

[18] Kevin Hsieh, Amar Phanishayee, Onur Mutlu, and Phillip Gibbons. The non-iid data quagmire of decentralized machine learning. In *Int. Conf. Machine Learn.*, pages 4387–4398. PMLR, 2020. 19

[19] Tzu-Ming Harry Hsu, Hang Qi, and Matthew Brown. Measuring the effects of non-identical data distribution for federated visual classification. *Neurips Workshop on Federated Learning*, 2019. 3, 6, 18

[20] Tzu-Ming Harry Hsu, Hang Qi, and Matthew Brown. Federated visual classification with real-world data distribution. In *Computer Vision–ECCV 2020: 16th European Conference, Glasgow, UK, August 23–28, 2020, Proceedings, Part X 16*, pages 76–92. Springer, 2020. 1, 6, 16, 18, 19

[21] Sergey Ioffe and Christian Szegedy. Batch normalization: Accelerating deep network training by reducing internal covariate shift. In *International conference on machine learning*, pages 448–456. PMLR, 2015. 19

[22] Pavel Izmailov, Dmitrii Podoprikhin, Timur Garipov, Dmitry Vetrov, and Andrew Gordon Wilson. Averaging weights leads to wider optima and better generalization. *Conference on Uncertainty in Artificial Intelligence*, 2018. 3

[23] Yiding Jiang, Behnam Neyshabur, Hossein Mobahi, Dilip Krishnan, and Samy Bengio. Fantastic generalization measures and where to find them. *ICLR*, 2019. 1

[24] Peter Kairouz, H Brendan McMahan, Brendan Avent, Aurélien Bellet, Mehdi Bennis, Arjun Nitin Bhagoji, Kallista

Bonawitz, Zachary Charles, Graham Cormode, Rachel Cummings, et al. Advances and open problems in federated learning. *Foundations and Trends® in Machine Learning*, 14(1–2):1–210, 2021. 1, 2

[25] Sai Praneeth Karimireddy, Martin Jaggi, Satyen Kale, Mehryar Mohri, Sashank J Reddi, Sebastian U Stich, and Ananda Theertha Suresh. Mime: Mimicking centralized stochastic algorithms in federated learning. *Advances in Neural Information Processing Systems*, 2020. 1, 3

[26] Sai Praneeth Karimireddy, Satyen Kale, Mehryar Mohri, Sashank Reddi, Sebastian Stich, and Ananda Theertha Suresh. Scaffold: Stochastic controlled averaging for federated learning. In *Int. Conf. Machine Learn.*, pages 5132–5143. PMLR, 2020. 1, 3, 5, 6, 16

[27] Nitish Shirish Keskar, Dheevatsa Mudigere, Jorge Nocedal, Mikhail Smelyanskiy, and Ping Tak Peter Tang. On large-batch training for deep learning: Generalization gap and sharp minima. *ICLR*, 2017. 1, 2

[28] Geeho Kim, Jinkyu Kim, and Bohyung Han. Communication-efficient federated learning with acceleration of global momentum. *arXiv preprint arXiv:2201.03172*, 2022. 3

[29] Alex Krizhevsky. Learning multiple layers of features from tiny images. Technical report, University of Toronto, 2009. 6

[30] Yann LeCun, Léon Bottou, Yoshua Bengio, and Patrick Haffner. Gradient-based learning applied to document recognition. *Proceedings of the IEEE*, 86(11):2278–2324, 1998. 6, 19

[31] Hao Li, Zheng Xu, Gavin Taylor, Christoph Studer, and Tom Goldstein. Visualizing the loss landscape of neural nets. *Advances in neural information processing systems*, 31, 2018. 20

[32] Li Li, Yuxi Fan, Mike Tse, and Kuo-Yi Lin. A review of applications in federated learning. *Computers & Industrial Engineering*, 149:106854, 2020. 1, 7

[33] Qinbin Li, Yiqun Diao, Quan Chen, and Bingsheng He. Federated learning on non-iid data silos: An experimental study. In *2022 IEEE 38th International Conference on Data Engineering (ICDE)*, pages 965–978. IEEE, 2022. 7

[34] Tian Li, Anit Kumar Sahu, Ameet Talwalkar, and Virginia Smith. Federated learning: Challenges, methods, and future directions. *IEEE signal processing magazine*, 37(3):50–60, 2020. 1

[35] Tian Li, Anit Kumar Sahu, Manzil Zaheer, Maziar Sanjabi, Ameet Talwalkar, and Virginia Smith. Federated optimization in heterogeneous networks. *Proceedings of Machine learning and systems*, 2:429–450, 2020. 1, 3, 6

[36] Xiang Li, Kaixuan Huang, Wenhao Yang, Shusen Wang, and Zhihua Zhang. On the convergence of fedavg on non-iid data. *ICLR*, 2020. 1, 2

[37] Quande Liu, Cheng Chen, Jing Qin, Qi Dou, and Pheng-Ann Heng. Feddg: Federated domain generalization on medical image segmentation via episodic learning in continuous frequency space. In *Proceedings of the IEEE/CVF Conference on Computer Vision and Pattern Recognition*, pages 1013–1023, 2021. 1, 2

[38] Yong Liu, Siqi Mai, Xiangning Chen, Cho-Jui Hsieh, and Yang You. Towards efficient and scalable sharpness-aware minimization. In *Proceedings of the IEEE/CVF Conference on Computer Vision and Pattern Recognition*, pages 12360–12370, 2022. 3

[39] Brendan McMahan, Eider Moore, Daniel Ramage, Seth Hampson, and Blaise Aguera y Arcas. Communication-efficient learning of deep networks from decentralized data. In *Artificial intelligence and statistics*, pages 1273–1282. PMLR, 2017. 1, 2, 3, 6

[40] Jiaxu Miao, Zongxin Yang, Leilei Fan, and Yi Yang. Fedseg: Class-heterogeneous federated learning for semantic segmentation. In *Proceedings of the IEEE/CVF Conference on Computer Vision and Pattern Recognition*, pages 8042–8052, 2023. 1, 2

[41] Theodora Nevrataki, Anastasia Iliadou, George Ntolkeras, Ioannis Sfakianakis, Lazaros Lazaridis, George Maraslidis, Nikolaos Asimopoulos, and George F Fragulis. A survey on federated learning applications in healthcare, finance, and data privacy/data security. In *AIP Conference Proceedings*. AIP Publishing, 2023. 1

[42] Jinseong Park, Hoki Kim, Yujin Choi, and Jaewook Lee. Differentially private sharpness-aware training. *Int. Conf. Machine Learn.*, 2023. 3, 5

[43] Adam Paszke, Sam Gross, Francisco Massa, Adam Lerer, James Bradbury, Gregory Chanan, Trevor Killeen, Zeming Lin, Natalia Gimelshein, Luca Antiga, Alban Desmaison, Andreas Kopf, Edward Yang, Zachary DeVito, Martin Raison, Alykhan Tejani, Sasank Chilamkurthy, Benoit Steiner, Lu Fang, Junjie Bai, and Soumith Chintala. Pytorch: An imperative style, high-performance deep learning library. In *Advances in Neural Information Processing Systems 32*, pages 8024–8035. Curran Associates, Inc., 2019. 19

[44] Henning Petzka, Michael Kamp, Linara Adilova, Cristian Sminchisescu, and Mario Boley. Relative flatness and generalization, 2021. 2

[45] Zhe Qu, Xingyu Li, Rui Duan, Yao Liu, Bo Tang, and Zhuo Lu. Generalized federated learning via sharpness aware minimization. In *Int. Conf. Machine Learn.*, pages 18250–18280. PMLR, 2022. 1, 2, 3, 4, 5, 6

[46] Ashish Rauniyar, Desta Haileselassie Hagos, Debesh Jha, Jan Erik Håkegård, Ulas Bagci, Danda B Rawat, and Vladimir Vlassov. Federated learning for medical applications: A taxonomy, current trends, challenges, and future research directions. *IEEE Internet of Things Journal*, 2023. 1

[47] Sashank Reddi, Zachary Charles, Manzil Zaheer, Zachary Garrett, Keith Rush, Jakub Konečnỳ, Sanjiv Kumar, and H Brendan McMahan. Adaptive federated optimization. *ICLR*, 2021. 1, 2, 3

[48] Jae Hun Ro, Ananda Theertha Suresh, and Ke Wu. FedJAX: Federated learning simulation with JAX. *arXiv preprint arXiv:2108.02117*, 2021. 19

[49] Sebastian Ruder. An overview of gradient descent optimization algorithms. *arXiv preprint arXiv:1609.04747*, 2016. 3

[50] Mark Sandler, Andrew Howard, Menglong Zhu, Andrey Zhmoginov, and Liang-Chieh Chen. Mobilenetv2: Inverted

residuals and linear bottlenecks. In *Proceedings of the IEEE conference on computer vision and pattern recognition*, pages 4510–4520, 2018. 6, 19

[51] Donald Shenaj, Eros Fanì, Marco Toldo, Debora Caldarola, Antonio Tavera, Umberto Michieli, Marco Ciccone, Pietro Zanuttigh, and Barbara Caputo. Learning across domains and devices: Style-driven source-free domain adaptation in clustered federated learning. In *Proceedings of the IEEE/CVF Winter Conference on Applications of Computer Vision*, pages 444–454, 2023. 1, 2

[52] Yifan Shi, Yingqi Liu, Kang Wei, Li Shen, Xueqian Wang, and Dacheng Tao. Make landscape flatter in differentially private federated learning. In *Proceedings of the IEEE/CVF Conference on Computer Vision and Pattern Recognition*, pages 24552–24562, 2023. 2

[53] Yan Sun, Li Shen, Shixiang Chen, Liang Ding, and Dacheng Tao. Dynamic regularized sharpness aware minimization in federated learning: Approaching global consistency and smooth landscape. *Int. Conf. Machine Learn.*, 2023. 1, 2, 4, 5, 6, 16, 18

[54] Yan Sun, Li Shen, Tiansheng Huang, Liang Ding, and Dacheng Tao. Fedspeed: Larger local interval, less communication round, and higher generalization accuracy. *ICLR*, 2023. 1, 2, 5, 6, 16, 18

[55] Ilya Sutskever, James Martens, George Dahl, and Geoffrey Hinton. On the importance of initialization and momentum in deep learning. In *Int. Conf. Machine Learn.*, pages 1139–1147. PMLR, 2013. 3

[56] Farshid Varno, Marzie Saghayi, Laya Rafiee Sevyeri, Sharut Gupta, Stan Matwin, and Mohammad Havaei. Adabest: Minimizing client drift in federated learning via adaptive bias estimation. In *European Conference on Computer Vision*, pages 710–726. Springer, 2022. 1, 2, 3, 4, 7

[57] Jie Wen, Zhixia Zhang, Yang Lan, Zhihua Cui, Jianghui Cai, and Wensheng Zhang. A survey on federated learning: challenges and applications. *International Journal of Machine Learning and Cybernetics*, 14(2):513–535, 2023. 1

[58] Tobias Weyand, Andre Araujo, Bingyi Cao, and Jack Sim. Google landmarks dataset v2-a large-scale benchmark for instance-level recognition and retrieval. In *Proceedings of the IEEE/CVF conference on computer vision and pattern recognition*, pages 2575–2584, 2020. 6

[59] Yuxin Wu and Kaiming He. Group normalization. In *Proceedings of the European conference on computer vision (ECCV)*, pages 3–19, 2018. 19

[60] Peng Xu, Bryan He, Christopher De Sa, Ioannis Mitliagkas, and Chris Re. Accelerated stochastic power iteration. In *International Conference on Artificial Intelligence and Statistics*, pages 58–67. PMLR, 2018. 20

[61] Riccardo Zaccone, Carlo Masone, and Marco Ciccone. Communication-efficient heterogeneous federated learning with generalized heavy-ball momentum. *arXiv preprint arXiv:2311.18578*, 2023. 3, 16, 18

[62] Tuo Zhang, Lei Gao, Chaoyang He, Mi Zhang, Bhaskar Krishnamachari, and A Salman Avestimehr. Federated learning for the internet of things: Applications, challenges, and opportunities. *IEEE Internet of Things Magazine*, 5(1):24–29, 2022. 1

Beyond Local Sharpness: Communication-Efficient Global Sharpness-aware Minimization for Federated Learning
Appendix

A. Algorithm

Alg. 1 summarizes FEDGLOSS, using as an example SGD or SAM as local optimizers, differently highlighted. The comment colors replicate those of Fig. 3.

Algorithm 1 FEDGLOSS with SAM or SGD as local optimizers

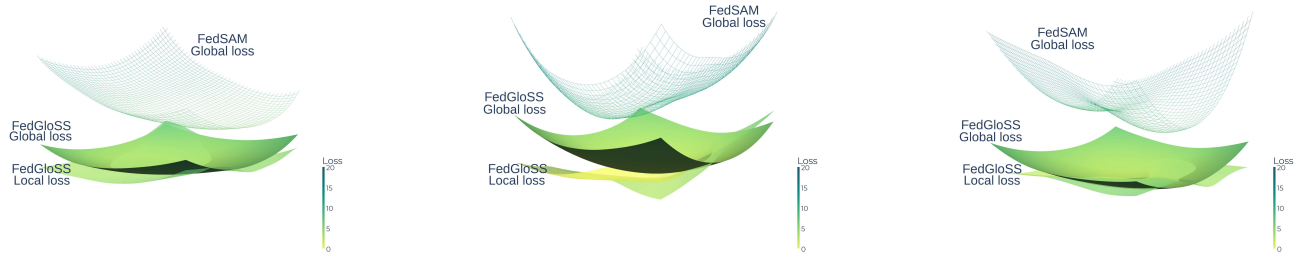
Input: Global model $\boldsymbol{w}$, clients $\mathcal{C}$, rounds T, local iterations E, clients' learning rate η, clients' SAM neighborhood size ρ_l, FEDGLOSS neighborhood size ρ, Lagrangian hyperparameter β.
Initialize: $\boldsymbol{w}^0$, $\sigma^0 = \sigma_k = 0$, $\Delta_{\boldsymbol{w}}^0 = 0$.
for each round $t \in [1, T]$ **do**
  $\tilde{\boldsymbol{\epsilon}}^t(\boldsymbol{w}) = \rho \frac{\Delta_{\boldsymbol{w}}^{t-1}}{\|\Delta_{\boldsymbol{w}}^{t-1}\|_2}$ ▷ Global perturbation with previous pseudo-grad
  $\tilde{\boldsymbol{w}}^t = \boldsymbol{w}^t + \tilde{\boldsymbol{\epsilon}}^t(\boldsymbol{w})$ ▷ Server-side approximated **FEDGLOSS ascent step**
  Randomly select a subset of clients $\mathcal{C}^t \subset \mathcal{C}$
  for each client $k \in \mathcal{C}^t$ in parallel **do**
    $\boldsymbol{w}_{k,0} = \tilde{\boldsymbol{w}}^t$ ▷ Initialize local model with *perturbed* global model $\tilde{\boldsymbol{w}}^t$
    Set iteration counter $i = 1$
    for each epoch $e \in [1, E]$ **do**
      for each batch $\mathcal{B} \in \mathcal{D}_k$ **do**
        $\boldsymbol{g}_{k,i} = \nabla f_{\mathcal{B}}(\boldsymbol{w}_{k,i-1})$ ▷ Local SGD gradient
        $\hat{\boldsymbol{\epsilon}}_{k,i} = \rho_l \frac{\boldsymbol{g}_{k,i}}{\|\boldsymbol{g}_{k,i}\|_2}$ ▷ SAM local perturbation
        $\boldsymbol{g}_{k,i} = \nabla f_{\mathcal{B}}(\boldsymbol{w}_{k,i-1} + \hat{\boldsymbol{\epsilon}}_{k,i})$ ▷ Local sharpness-aware gradient
        $\boldsymbol{w}_{k,i} \leftarrow \boldsymbol{w}_{k,i-1} - \eta[\boldsymbol{g}_{k,i} - \sigma_k + (\boldsymbol{w}_{k,i-1} - \boldsymbol{w}_{k,0})/\beta]$ ▷ Local update with ADMM
        $i \leftarrow i + 1$
      end for
    end for
    $\sigma_k \leftarrow \sigma_k - (\boldsymbol{w}_{k,E} - \tilde{\boldsymbol{w}}^t)/\beta$ ▷ Update local dual variable
    Send back to the server the local updated model $\boldsymbol{w}_k^t = \boldsymbol{w}_{k,E}$
  end for
  $\sigma^{t+1} = \sigma^t - \frac{1}{\beta|\mathcal{C}|} \sum_{k \in \mathcal{C}} (\boldsymbol{w}_k^t - \tilde{\boldsymbol{w}}^t)$ ▷ Update global dual variable
  $\tilde{\Delta}_{\boldsymbol{w}}^t = \sum_{k \in \mathcal{C}^t} \frac{N_k}{N} (\tilde{\boldsymbol{w}}^t - \boldsymbol{w}_k^t)$ ▷ **Global pseudo-gradient**
  $\boldsymbol{w}^{t+1} = \boldsymbol{w}^t - \tilde{\Delta}_{\boldsymbol{w}}^t - \beta\sigma^{t+1}$ ▷ FEDGLOSS descent step w/ pseudo-grad using ADMM
end for

B. The Benefits on FEDGLOSS

B.1. Achieving Consistency on Local and Global Sharpness with FedGloSS

This section completes the analyses presented in Secs. 4 and 6.2, showing how FEDGLOSS guides towards consistent local and global flat loss landscapes. Fig. 10 extends Figs. 4a and 4b from the main paper with the 3 remaining clients (out of 5) selected in the last round, comparing the behavior of clients' models trained with FEDGLOSS from the local and global perspectives. These results highlight the effectiveness of FEDGLOSS in achieving local models with consistent local-global behavior. Indeed, these models end up in flat regions both in local and global loss landscapes. The comparison with FEDSAM (*net* surface) further demonstrates the effectiveness of using our global flatness-aware approach.

Fig. 11 instead extends Figs. 4c and 4d, offering a comparative analysis of FEDSMOO's clients' models w.r.t. FEDGLOSS (*net* landscape). The local solutions found by FEDGLOSS achieve flatter, better (*i.e.*, lower loss) and more consistent convergence points in the *global* loss landscape w.r.t. our main competitor FEDSMOO.

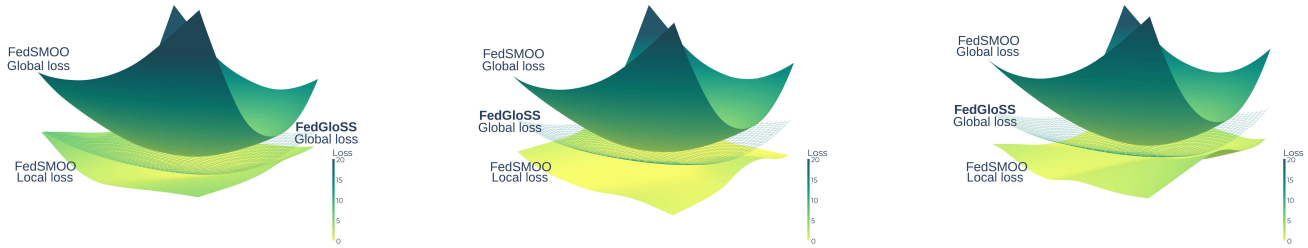


(a) Local model trained on class `bear` with FEDGLOSS

(b) Local model trained on class `skyscraper` with FEDGLOSS

(c) Local model trained on class `possum` with FEDGLOSS

Figure 10. **Global *vs.* local perspective on FEDGLOSS**. CIFAR100 $\alpha = 0$ with SAM as local optimizer @ $20k$ rounds on CNN. **(a) - (c):** Local models trained on one `class`, tested on the local ("*Local loss*") or global dataset ("*Global loss*"). Corresponding global perspective of local model trained with FEDSAM (*net*) added as reference.

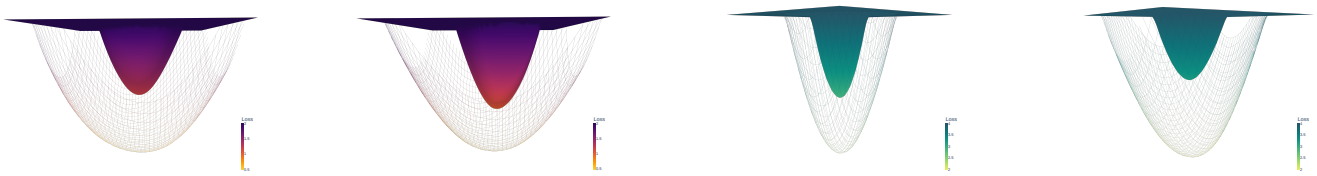


(a) Local model trained on class `bear` with FEDGLOSS

(b) Local model trained on class `skyscraper` with FEDGLOSS

(c) Local model trained on class `possum` with FEDGLOSS

Figure 11. **Global *vs.* local perspective on FEDSMOO**. CIFAR100 $\alpha = 0$ with SAM as local optimizer @ $20k$ rounds on CNN. **(a) - (c):** Local models trained on one `class`, tested on the local ("*Local loss*") or global dataset ("*Global loss*"). Corresponding global perspective of local model trained with FEDGLOSS (*net*) added as reference.

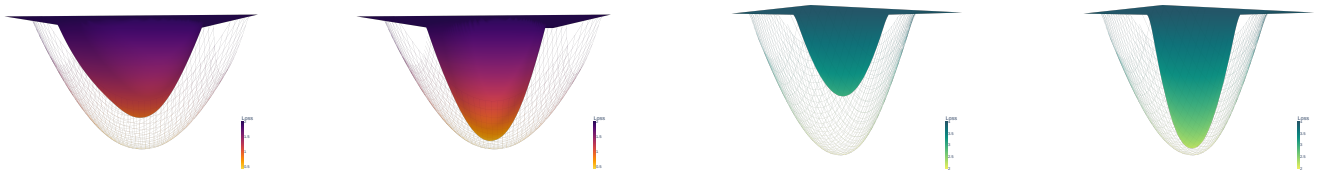


(a) CIFAR10 $\alpha = 0$ (b) CIFAR10 $\alpha = 0.05$ (c) CIFAR100 $\alpha = 0$ (d) CIFAR100 $\alpha = 0.5$

Figure 12. Visualization of the loss landscapes of the CNN trained with **FEDGLOSS** (*net*) and the de-facto standard optimization algorithm in FL **FEDAVG** (*solid*). Comparison with varying degrees of heterogeneity on CIFAR10 (left) and CIFAR100 (right). **FEDGLOSS consistently achieves flatter minima and lower loss values in the *global* loss landscape.**

B.2. Achieving Flatter Global Minima

FEDGLOSS *vs.* FEDAVG, FEDSAM, FEDSMOO. Fig. 12 compares the loss landscapes of global models trained with FEDGLOSS and FEDAVG, showing how the former consistently achieves flatter minima and lower loss values in the *global* loss landscapes. This confirms the behaviors already appreciated in Fig. 6. In addition, Fig. 13 shows the global loss surfaces of FEDGLOSS' solutions against models trained with FEDSAM and FEDSMOO. These plots extend Fig. 6 with the less heterogeneous scenarios $\alpha = 0.05$ for CIFAR10 and $\alpha = 0.5$ on CIFAR100. They confirm FEDGLOSS' effectiveness in reaching flatter and lower-loss solutions with respect to its main direct competitors.



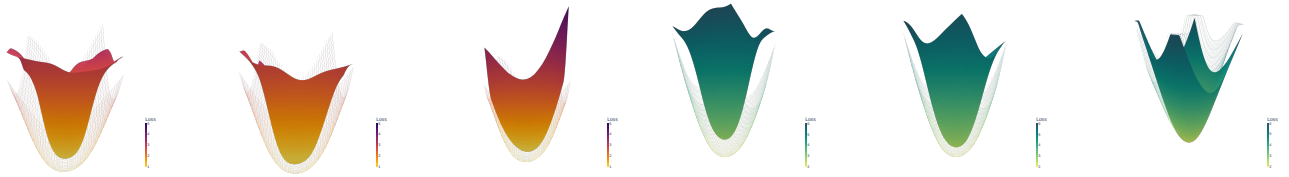
(a) CIFAR10 $\alpha = 0.05$ FEDGLOSS *vs.* FEDSAM

(b) CIFAR10 $\alpha = 0.05$ FEDGLOSS *vs.* FEDSMOO

(c) CIFAR100 $\alpha = 0.5$ FEDGLOSS *vs.* FEDSAM

(d) CIFAR100 $\alpha = 0.5$ FEDGLOSS *vs.* FEDSMOO

Figure 13. Visualization of the loss landscapes of the CNN trained with **FEDGLOSS** (*net*) **and FEDSAM or FEDSMOO** (*solid*). Comparison with $\alpha = 0.05$ CIFAR10 (left) and $\alpha = 0.5$ CIFAR100 (right) extending Fig. 6. **FEDGLOSS consistently achieves flatter minima and lower loss values in the *global* loss landscape.**



(a) CIFAR10 $\alpha = 0.05$ FEDGLOSS (*net*) *vs.* FEDAVG (*solid*)

(b) CIFAR10 $\alpha = 0.05$ FEDGLOSS (*net*) *vs.* FEDSAM (*solid*)

(c) CIFAR10 $\alpha = 0.05$ FEDGLOSS (*net*) *vs.* FEDSMOO (*solid*)

(d) CIFAR100 $\alpha = 0.5$ FEDGLOSS (*net*) *vs.* FEDAVG (*solid*)

(e) CIFAR100 $\alpha = 0.5$ FEDGLOSS (*net*) *vs.* FEDSAM (*solid*)

(f) CIFAR100 $\alpha = 0.5$ FEDGLOSS (*net*) *vs.* FEDSMOO (*solid*)

Figure 14. Visualization of loss landscapes of the ResNet18 trained with **FEDGLOSS** (*net*) **and FEDAVG, or FEDSAM or FEDSMOO** (*solid*). Comparison with CIFAR10 $\alpha = 0.05$ (*a-c*) and CIFAR100 $\alpha = 0.5$ (*d-f*). **FEDGLOSS achieves flatter and lower-loss regions in the global landscape**.

FEDGLOSS on ResNet18. Fig. 14 extends Fig. 6 from the main paper and shows the flatter loss landscapes reached by FEDGLOSS when using ResNet18 on CIFAR10 and CIFAR100.

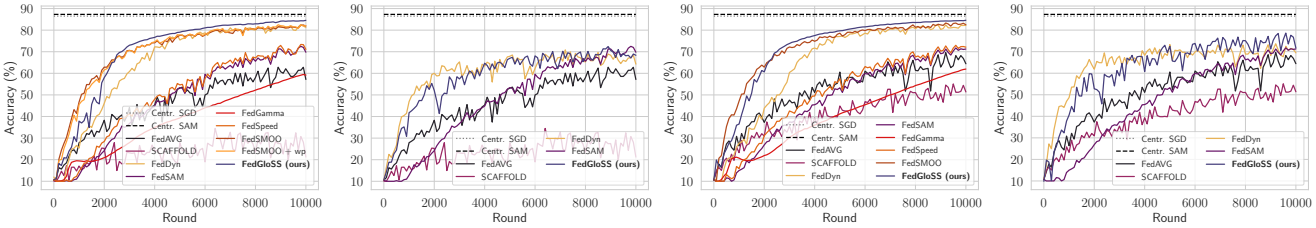
Hessian Eigenvalues. Tab. 9 reports the values of the maximum Hessian eigenvalues, as already shown in Fig. 7 in the main paper. First, as expected, we note that SAM-based methods achieve flatter minima w.r.t. the counterpart. Notably, our main competitor FEDSMOO presents higher sharpness than FEDSAM in the simpler CIFAR10, regardless of the data distribution. In addition, FEDGLOSS with local SAM achieves the lowest sharpness (*i.e.*, lowest λ_1) on *all* configurations, outperforming the state of the art and, specifically, *all* sharpness-aware methods.

Table 9. **FEDGLOSS *vs.* the state of the art**, distinguished by local optimizer - SGD (*top*) and SAM (*bottom*). Comparison in terms of communication cost and maximum Hessian eigenvalue λ_1. Best results in **bold**. Model: CNN.

	Method	Comm. Cost	CIFAR10 $\alpha = 0$ $\lambda_1(\downarrow)$	CIFAR10 $\alpha = 0.05$ $\lambda_1(\downarrow)$	CIFAR100 $\alpha = 0$ $\lambda_1(\downarrow)$	CIFAR100 $\alpha = 0.5$ $\lambda_1(\downarrow)$
Client SGD	FEDAVG	1×	66.23 ± 0.50	71.14 ± 4.07	$\mathbf{66.30 \pm 3.08}$	68.77 ± 0.96
	FEDPROX	1×	66.19 ± 0.52	71.41 ± 4.40	66.34 ± 3.75	$\mathbf{68.63 \pm 1.37}$
	FEDDYN	1×	63.94 ± 4.41	71.44 ± 8.73	-	-
	SCAFFOLD	2×	166.54 ± 6.93	180.51 ± 30.08	-	120.01 ± 0.76
	FEDGLOSS	1×	$\mathbf{58.26 \pm 3.49}$	$\mathbf{56.28 \pm 4.19}$	96.01 ± 9.00	107.35 ± 7.5
Client SAM	FEDSAM	1×	10.35 ± 0.07	9.43 ± 0.28	58.38 ± 2.93	57.54 ± 1.21
	FEDDYN	1×	10.04 ± 5.38	6.58 ± 0.20	-	-
	FEDSPEED	1×	10.92 ± 0.17	9.97 ± 0.12	58.23 ± 3.18	58.00 ± 1.86
	FEDGAMMA	2×	4.79 ± 0.20	4.55 ± 0.20	-	99.86 ± 6.74
	FEDSMOO	2×	15.37 ± 1.67	12.57 ± 0.56	28.43 ± 1.97	29.23 ± 0.17
	FEDGLOSS	1×	$\mathbf{2.03 \pm 0.05}$	$\mathbf{1.93 \pm 0.03}$	$\mathbf{17.18 \pm 0.97}$	$\mathbf{16.22 \pm 0.35}$

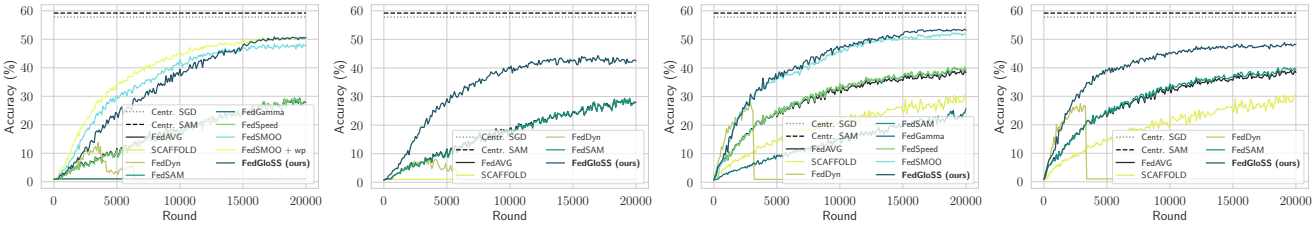
B.3. Increasing Convergence Speed

Figs. 15 and 16 show the accuracy trends of FEDGLOSS compared to state-of-the-art methods for heterogeneous FL on CIFAR10 and CIFAR100 respectively. For a clearer understanding, we distinguish between SAM-based and SGD-based



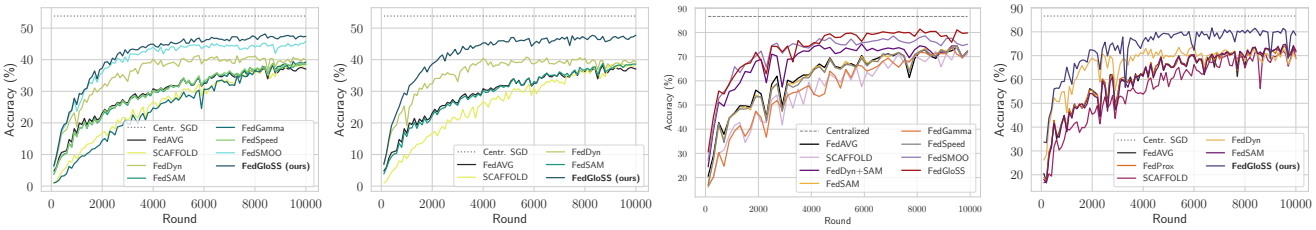
(a) $\alpha = 0$ SAM (b) $\alpha = 0$ SGD (c) $\alpha = 0.05$ SAM (d) $\alpha = 0.05$ SGD

Figure 15. CIFAR10 with varying degrees of heterogeneity ($\alpha \in \{0, 0.05\}$). Results of centralized runs (*dashed lines*) added as reference. Comparison of FEDGLOSS with state-of-the-art approaches, distinguished in SAM-based methods (**a**, **c**) and SGD-based ones (**b**, **d**). FEDGLOSS consistently achieves the best performance. Model: CNN.



(a) $\alpha = 0$ SAM (b) $\alpha = 0$ SGD (c) $\alpha = 0.5$ SAM (d) $\alpha = 0.5$ SGD

Figure 16. CIFAR100 with varying degrees of heterogeneity ($\alpha \in \{0, 0.5\}$) with **CNN**. Results of centralized runs (*dashed lines*) added as reference. Comparison of FEDGLOSS with state-of-the-art approaches, distinguished in SAM-based methods (**a**, **c**) and SGD-based ones (**b**, **d**). FEDGLOSS consistently achieves the best performance.



(a) CIFAR100 $\alpha = 0.5$ SAM (b) CIFAR100 $\alpha = 0.5$ SGD (c) CIFAR10 $\alpha = 0.05$ SAM (d) CIFAR10 $\alpha = 0.05$ SGD

Figure 17. Accuracy trends with **ResNet18** on CIFAR100 (*left*) and CIFAR10 (*right*). Comparison of FEDGLOSS with state-of-the-art approaches, distinguished in SAM-based methods (**a**, **c**) and SGD-based ones (**b**, **d**). FEDGLOSS consistently achieves the best performance, both in terms of final accuracy and convergence speed.

methods depending on the used local optimizer. For a fair comparison, we report FEDSMOO with and without the scheduling of ρ (+*wp* in the figure). For additional details on the scheduling, refer to App. C. FEDGLOSS consistently achieves the best performances and convergence speedup in each group. In addition, we remind that FEDGLOSS communicates *half* the number of bits at each round w.r.t. FEDSMOO. Fig. 17 reports the results obtained with ResNet18 on both datasets: FEDGLOSS consistently achieves the best speed of convergence and final accuracy, with both SAM and SGD as CLIENTOPT.

B.4. Effectiveness in Multiple Scenarios and with Several Model Architectures

As already shown in Sec. 6, FEDGLOSS outperforms the state of the art in terms of speed of convergence, final performance in accuracy, flatness of the solution and communication efficiency. This remains true across multiple datasets (CIFAR100, CIFAR10, LANDMARKS-USER-160K) and model architectures (CNN, ResNet18, MobileNetv2). The main paper focuses on results in more challenging heterogeneous FL scenarios. The next paragraphs discuss the behavior of FEDGLOSS in increasingly more homogeneous settings.

Table 10. FEDGLOSS against SOTA algorithms in increasingly more homogeneous settings on CIFAR10, compared in terms of accuracy (%) and maximum Hessian eigenvalue λ_1. Best results in **bold**. Model: CNN.

	Method	$\alpha = 1$		$\alpha = 5$		$\alpha = 10$	
		Accuracy	λ_1	Accuracy	λ_1	Accuracy	λ_1
SGD-based	FEDAVG	76.4 ± 0.2	68.2 ± 2.7	83.7 ± 0.4	63.3 ± 2.9	82.4 ± 0.1	70.6 ± 0.3
	FEDPROX	76.3 ± 0.2	69.5 ± 0.9	83.8 ± 0.4	63.0 ± 3.6	82.4 ± 0.2	71.8 ± 2.0
	FEDDYN	77.1 ± 0.1	64.5 ± 4.9	82.3 ± 0.3	48.3 ± 1.6	82.2 ± 0.1	58.1 ± 3.5
	SCAFFOLD	79.6 ± 0.1	62.7 ± 2.7	$\mathbf{84.5 \pm 0.2}$	47.4 ± 3.0	83.8 ± 0.2	58.4 ± 2.9
	FEDGLOSS	$\mathbf{80.31 \pm 0.4}$	$\mathbf{40.0 \pm 5.2}$	83.5 ± 0.2	$\mathbf{8.5 \pm 0.3}$	$\mathbf{84.8 \pm 0.3}$	$\mathbf{41.4 \pm 2.2}$
SAM-based	FEDSAM	77.7 ± 0.2	25.6 ± 0.02	83.5 ± 0.1	19.7 ± 0.1	83.2 ± 0.2	22.1 ± 1.4
	FEDDYN	80.5 ± 0.2	21.0 ± 0.8	82.9 ± 0.4	16.3 ± 0.5	84.1 ± 0.1	17.3 ± 0.3
	FEDSPEED	76.2 ± 0.5	8.3 ± 0.1	83.6 ± 0.1	20.3 ± 0.5	78.2 ± 0.2	8.6 ± 0.2
	FEDGAMMA	70.3 ± 1.0	4.8 ± 0.2	83.5 ± 0.1	16.0 ± 0.6	76.4 ± 0.3	6.4 ± 0.1
	FEDSMOO	85.2 ± 0.2	9.8 ± 0.2	86.2 ± 0.2	6.0 ± 0.2	86.8 ± 0.3	6.2 ± 0.2
	FEDGLOSS	$\mathbf{85.6 \pm 0.2}$	$\mathbf{2.0 \pm 0.04}$	$\mathbf{86.9 \pm 0.2}$	$\mathbf{4.5 \pm 0.02}$	$\mathbf{87.1 \pm 0.1}$	$\mathbf{4.1 \pm 0.03}$

FEDGLOSS in moderately heterogeneous settings. The choice of the Dirichlet's concentration parameter α in the main text aligns with the FL literature [1, 4, 20, 53, 54], where $\alpha < 1$ is commonly used to evaluate challenging settings. Moreover, for $\alpha > 0.6$, differences between methods become less pronounced [61]. To further analyze the impact of varying heterogeneity levels on FEDGLOSS, we consider $\alpha \in \{1, 5, 10\}$ on CIFAR10. Tab. 10 presents a comparison of FEDGLOSS against several state-of-the-art FL algorithms. Consistently, FEDGLOSS achieves the highest accuracy across all tested scenarios, except for $\alpha = 5$ with SGD as the local optimizer, where it is outperformed by SCAFFOLD. Notably, even in this case, FEDGLOSS exhibits the lowest maximum Hessian eigenvalue, highlighting its stability.

FEDGLOSS in homogeneous settings. Tab. 11 evaluates FEDGLOSS against the main methods FEDAVG, FEDSAM, FEDDYN and FEDSMOO in homogeneous FL settings. Here, client gradients are naturally more aligned due to reduced client drift [26]. We thus test FEDGLOSS with and without ADMM for global consistency. As expected, FEDGLOSS achieves similar accuracy with or without ADMM, particularly when using SAM as the local optimizer. However, ADMM facilitates convergence to flatter minima (evidenced by lower λ_1 values) by aligning local and global convergence points. Notably, FEDGLOSS achieves the flattest minima (lowest λ_1) across both datasets, and the best accuracy on the more complex CIFAR100. While FEDSMOO achieves slightly higher accuracy on CIFAR10, FEDGLOSS finds a flatter minimum and achieves competitive accuracy with significantly lower communication costs (halved).

Table 11. FEDGLOSS against SOTA FL methods on homogeneous CIFAR settings, compared in terms of communication costs, accuracy (%) and maximum Hessian eigenvalue λ_1. Best result in **bold** and second best underlined. Model: CNN.

Method	Comm. Cost	ADMM	CIFAR10 $\alpha = 100$		CIFAR100 $\alpha = 1000$	
			Accuracy	λ_1	Accuracy	λ_1
FEDAVG	$1\times$	✗	84.0	68.4	50.1	49.4
FEDSAM	$1\times$	✗	84.7	36.2	53.4	32.6
FEDDYN (SGD)	$1\times$	✓	83.8	47.8	51.9	91.7
FEDDYN (SAM)	$1\times$	✓	84.5	27.9	52.5	46.0
FEDSMOO	$2\times$	✓	**85.1**	<u>6.4</u>	53.9	24.6
FEDGLOSS (SGD)	$1\times$	✗	84.0	67.7	50.5	50.8
	$1\times$	✓	83.1	7.1	51.7	47.9
FEDGLOSS (SAM)	$1\times$	✗	<u>84.8</u>	36.2	**55.8**	<u>13.9</u>
	$1\times$	✓	<u>84.8</u>	**2.8**	<u>55.7</u>	**11.8**

B.5. Reducing Communication Costs

Analysis on communication cost. Tab. 12 extends the analysis presented in Sec. 6.3.4 by evaluating the communication costs across all scenarios considered in this work. Notably, since FEDGLOSS maintains the per-round communication cost of FEDAVG, it remains advantageous even when matching the convergence speed of the best-performing algorithm (FEDSMOO), due to its *halved communication costs*.

Table 12. Communication costs comparison w.r.t. FEDAVG. "-" for not reached accuracy, "✗" for non-convergence.

	Method	CNN								ResNet18				MobileNetv2	
		CIFAR-10				CIFAR-100				CIFAR-10		CIFAR-100		LANDMARKS-USER-160K	
		$\alpha = 0$		$\alpha = 0.05$		$\alpha = 0$		$\alpha = 0.5$		$\alpha = 0.05$		$\alpha = 0.5$			
		Rounds	*Cost*	*Rounds*	*Cost*	*Rounds*	*Cost*	*Rounds*	*Cost*	*Rounds*	*Cost*	*Rounds*	*Cost*	*Rounds*	*Cost*
SGD-based	FEDAVG	$10k$ (1×)	$1B$	$10k$ (1×)	$1B$	$20k$ (1×)	$1B$	$20k$ (1×)	$1B$	$10k$ (1×)	$1B$	$10k$ (1×)	$1B$	$1.3k$ (1×)	$1B$
	FEDPROX	$7.6k$ (1.3×)	$0.8B$	$7.9k$ (1.3×)	$0.8B$	$18.7k$ (1.1×)	$0.9B$	$18.6k$ (1.1×)	$0.9B$	$8.8k$ (1.1×)	$0.9B$	$8.3k$(1.2×)	$0.8B$	-	-
	FEDDYN	$2k$ (5×)	$\mathbf{0.2B}$	$1.9k$ (5×)	$\mathbf{0.2B}$	✗		✗		-	-	$3.5k$ (2.9×)	$0.4B$	-	-
	SCAFFOLD	-	-	-	-	-	-	-	-	-	-	$8.9k$ (1.1×)	$1.8B$	✗	
	FEDGLOSS	$3.4k$ (2.9×)	$0.3B$	$3.8k$ (2.6×)	$0.4B$	$5k$ (4×)	$\mathbf{0.3B}$	$4.7k$ (4.3×)	$\mathbf{0.2B}$	$2.4k$ (4.2×)	$\mathbf{0.2B}$	$1.9k$ (5.3×)	$\mathbf{0.2B}$	-	-
SAM-based	FEDSAM	$6.3k$ (1.6×)	$0.6B$	$7.8k$ (1.3×)	$0.8B$	$18.3k$ (1.1×)	$0.9B$	$16.3k$ (1.2×)	$0.8B$	$9.2k$ (1.1×)	$0.9B$	$7.8k$ (1.3×)	$0.8B$	$1.3k$ (1×)	$1B$
	FEDDYN	$3k$ (3.3×)	$0.3B$	$4.2k$ (2.4×)	$0.4B$	✗		✗		$4.1k$ (2.4×)	$0.4B$	$3.5k$ (2.9×)	$0.4B$	-	-
	FEDSPEED	$6.3k$ (1.6×)	$0.6B$	$6.9k$ (1.4×)	$0.7B$	$18.3k$ (1.1×)	$0.9B$	$15.7k$ (1.3×)	0.8B	$8.3k$ (1.2×)	$0.8B$	$8.3k$ (1.2×)	$0.8B$	$1.3k$ (1×)	$1B$
	FEDGAMMA	-	-	-	-	-	-	-	-	$9.3k$ (1.1×)	$1.9B$	$8.1k$ (1.2×)	$1.6B$	✗	
	FEDSMOO	$1.9k$ (5.3×)	$0.4B$	$2.2k$ (4.5×)	$0.4B$	$4.5k$ (4.4×)	$0.5B$	$6.5k$ (3.1×)	$0.7B$	$2.4k$ (4.2×)	$0.5B$	$2.3k$ (4.3×)	$0.5B$	200 (6.5×)	$0.3B$
	FEDGLOSS	$2.2k$ (4.5×)	$\mathbf{0.2B}$	$2.2k$ (4.5×)	$\mathbf{0.2B}$	$6.3k$ (3.2×)	$\mathbf{0.3B}$	$5.2k$ (3.8×)	$\mathbf{0.3B}$	$2.4k$ (4.2×)	$\mathbf{0.2B}$	$1.9k$ (5.3×)	$\mathbf{0.2B}$	200 (6.5×)	$\mathbf{0.2B}$

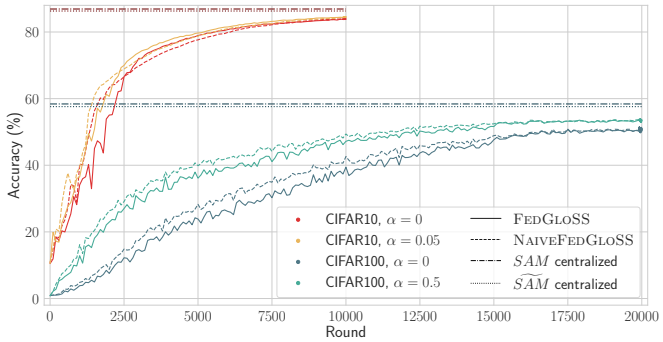


Figure 18. **Accuracy trends of FEDGLOSS *vs.* NAIVEFEDGLOSS.** The comparison includes the centralized upper bounds of SAM and $\widetilde{\text{SAM}}$ (the adaptation of FEDGLOSS' strategy to the centralized scenario). CNN on CIFAR10 and CIFAR100 with varying heterogeneity degree (α). NAIVEFEDGLOSS is $\approx 1.1\times$ faster than its efficient alternative FEDGLOSS in CIFAR100, while FEDGLOSS shows increased convergence speed after $\approx 25\%$ of training rounds in CIFAR10. However, both methods reach the same accuracy at the of training. These results motivate the choice of FEDGLOSS over NAIVEFEDGLOSS.

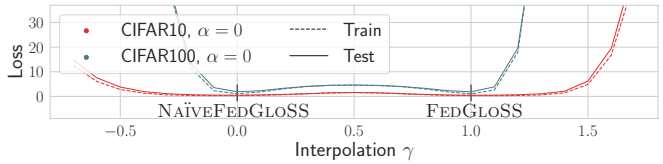


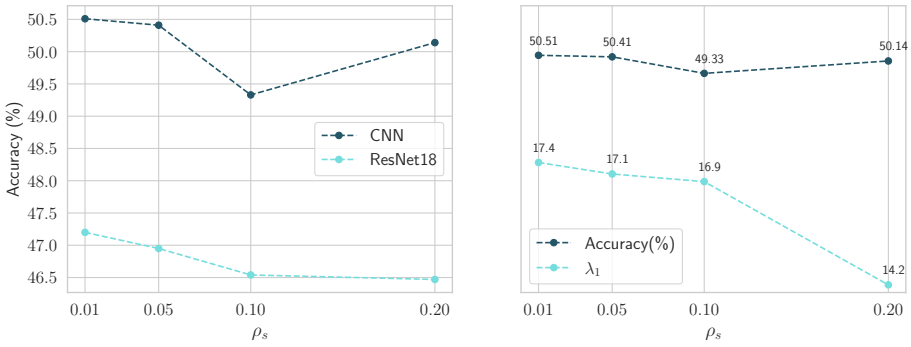
Figure 19. **Loss barriers** resulting from interpolating NAIVEFEDGLOSS and FEDGLOSS' models, which are found in the same basin. CIFAR datasets, CNN. Details on the computation in App. D.2.

FEDGLOSS *vs.* NAIVEFEDGLOSS. Fig. 18 deepens the comparison between FEDGLOSS and its baseline NAIVEFEDGLOSS, discussed in Sec. 6.4. In particular, this plot reports the accuracy trends of the two methods, showing that NAIVEFEDGLOSS is slightly faster ($\approx 1.1\times$) than FEDGLOSS in CIFAR100, while FEDGLOSS surpasses the speed of the baseline after $\approx 25\%$ of training in CIFAR10. However, both methods reach the same accuracy at the of training. In addition, it is to be noted that FEDGLOSS *halves* the communication cost w.r.t. NAIVEFEDGLOSS by transmitting half the number of bits at each round, as it eliminates the need to invoke the clients twice to compute the updates. Lastly, our sharpness approximation does not steer the optimization path: models trained with FEDGLOSS and NAIVEFEDGLOSS end up in the same basin (no loss barrier), with similar flatness (Fig. 19). These insights further support our choice of the efficient strategy of FEDGLOSS over NAIVEFEDGLOSS.

Convergence speed. Since all methods are compared over a fixed amount of communication rounds, **higher final accuracy implies faster convergence**. Since FEDGLOSS consistently outperforms the other state-of-the-art algorithms taken into account, it is guaranteed to converge faster, as also shown in the accuracy trends (Figs. 15 to 17).

B.6. The Impact of Server-side ρ_s

Fig. 20 analyzes the impact of ρ_s on the performance of the global model, both in terms of accuracy (Fig. 20a) and flatness of the solution (Fig. 20b). In details, Fig. 20a compares the accuracy of the global model trained on CIFAR100 when varying the model architecture (CNN *vs.* ResNet18) and the data heterogeneity ($\alpha = 0$ *vs.* $\alpha = 0.5$). In all the configurations, we note that a smaller value of ρ_s usually leads to the best results. Fig. 20b instead focuses on the CNN in the most heterogeneous setting ($\alpha = 0$) and compares the reached accuracy with the corresponding maximum Hessian eigenvalue λ_1 when varying ρ_s. A larger server-side ρ_s corresponds to a smaller λ_1, *i.e.*, a flatter region in the global loss landscape.



(a) FEDGLOSS ρ_s with different architectures

(b) FEDGLOSS ρ_s *vs.* λ_1

Figure 20. CIFAR100. **(a):** Accuracy (%) of FEDGLOSS when varying the server-side SAM ρ_s, with different heterogeneity and architecture (CNN with $\alpha = 0$ and ResNet18 with $\alpha = 0.5$). Smaller values of ρ_s lead to better performances. **(b):** FEDGLOSS ρ_s *vs.* maximum Hessian eigenvalue λ_1 on CNN with $\alpha = 0$. Larger values of ρ_s lead to lower eigenvalues with minimum loss in accuracy.

C. Implementation Details

This section delves into a comprehensive description of the datasets and models utilized throughout this paper, specifying the Deep Learning framework and the hardware employed (App. C.1). Additionally, we present the area of the hyper-parameters' space explored during the fine-tuning process in order to yield optimal results (App. C.2).

C.1. Datasets and Models

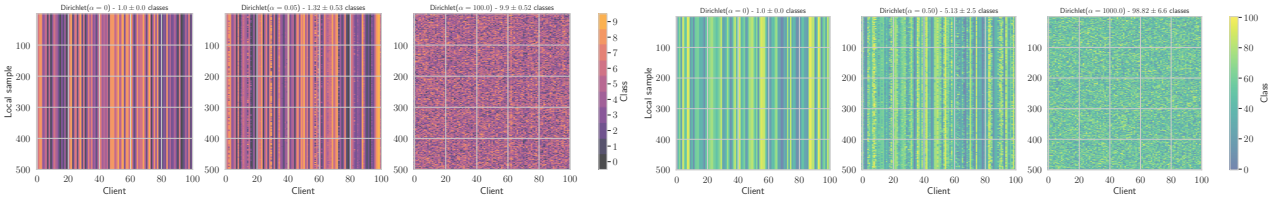
Tab. 13 provides a comprehensive overview of each dataset's general statistics. This includes the number of training clients participating in the process and the total number of samples used to construct both the training and test sets.

C.1.1. CIFAR10 and CIFAR100

We adapted these two well-known image classification datasets to the FL scenario by replicating the splits among clients proposed by [19]. Both datasets are split evenly among 100 clients, thus each of them has access to 500 data samples. This partitioning is performed according to a Latent Dirichlet Allocation (LDA) on the labels. In practice, each local dataset follows a multinomial distribution drawn according to a symmetric Dirichlet distribution with concentration parameter α. The higher the value of this parameter is, the more the local datasets resemble a homogeneous scenario, in the limit case $\alpha = 0$ each client has access to one only class of images. In our experiments we tested $\alpha \in \{0, 0.05, 1, 5, 10, 100\}$ and $\alpha \in \{0, 0.5, 1000\}$ for CIFAR10 and CIFAR100, respectively. Our choice of α aligns with FL literature [1, 4, 20, 53, 54], where $\alpha < 1$ is standard for testing challenging settings. Also, for $\alpha > 0.6$, method differences are less apparent [61]. Figs. 21a and 21b show how data is distributed across clients in all the experimental settings for these two datasets. Both datasets are pre-processed by applying random crops and random horizontal flips.

Table 13. Datasets' description with their general statistics on the size and number of clients.

Dataset	Train clients	Train samples	Test samples
CIFAR10	100	50,000	10,000
CIFAR100	100	50,000	10,000
LANDMARKS-USER-160K	1262	164,172	19,526



(a) CIFAR10 (b) CIFAR100

Figure 21. CIFAR10 (*left*) and CIFAR100 (*right*) data distribution across clients with the heterogeneity levels tested in the experiments. On top of each chart we report the average number of classes seen by each client.

Models. We trained a Convolutional Neural Network (CNN) inspired by the LeNet-5 architecture [30], as proposed by [20]. The network comprises two 64-channels convolutional layers, both using 5×5 kernels and followed by 2×2 max-pooling layers. This is succeeded by two fully-connected layers with 384 and 192 units, respectively. The final output layer is adapted to the specific number of classes in the dataset.

To explore deeper and more expressive architectures, we also trained a ResNet18 [16] on CIFAR100 with $\alpha = 0.5$ and CIFAR10 with $\alpha = 0.05$. We replaced the standard Batch Normalization layers [21] with Group Normalization layers [59] due to their demonstrated effectiveness in handling skewed data distributions in FL [18]. We carried out the experiments with the CNN model using PyTorch [43] and the ResNet18 ones using FedJAX [48].

C.1.2. LANDMARKS-USER-160K

To achieve a comprehensive understanding of the efficacy of the proposed method, a thorough analysis was undertaken utilizing large-scale real-world datasets. Specifically, we use the LANDMARKS-USER-160K dataset [20], a repository encompassing 164,172 images depicting 2028 distinct landmarks, distributed among 1262 clients.

Models. The model employed for training is a MobileNetV2 [20, 50], replacing batch normalization with group normalization layers and pre-trained on ImageNet [8]. The tests on this dataset were carried out on a cluster of NVIDIA A100 40GB, using our FedJAX codebase.

C.2. Hyperparameters

Grid search. In Tab. 14 we report the training hyperparameters associated to each dataset and model pairing, while Tab. 15 summarizes the hyper-parameters search grid tested for each method (in bold the chosen ones). All runs are averaged over 3 seeds. In addition, following previous works [1, 4, 5], we report the averaged accuracy of the last 100 rounds to reduce the noise typical of heterogeneous FL settings.

Local hyperparameters. As for local hyperparameters, we tested FEDGLOSS' robustness to $E = 2$ and $\eta_l = 0.001$ on CIFAR10 with $\alpha = 0$. A smaller η_l had the greatest impact, with FEDAVG and FEDSAM losing 45% and 77% of their performance (more local steps degrade performance in heterogeneous settings), respectively. Notably, FEDGLOSS loses only 29%. We attribute this to the pseudo-gradient consistently pointing toward higher-loss regions, ensuring a reliable ascent step approximation regardless of local hyperparameters.

Scheduling of ρ. While running our experiments on FEDGLOSS, we noticed that a larger value of local ρ allowed to reach the best final accuracy, while a smaller ρ achieved faster convergence in the initial training stages. Following this insight, we schedule the value of ρ for T_s rounds as

$$\rho(t) = \begin{cases} \rho_0 + {}^{(\rho-\rho_0)}/_{T_s} \cdot t & \text{if } t \leq T_s \\ \rho & \text{otherwise,} \end{cases}$$

starting from the value $\rho_0 = 0.001$.

D. Flatness Analysis

This section describes the procedure to compute the visualization of the loss landscapes and the Hessian eigenvalues.

Table 14. General training hyper-parameters common to all methods, distinguished by dataset and model architecture. Symbols: local epochs E, local learning rate η, weight decay wd, client-side momentum β_l, batch size B.

Dataset	Model	Rounds	Clients per round	Client optimization				
				E	η	wd	β_l	B
CIFAR10	CNN	10000	5	1	10^{-2}	$4 \cdot 10^{-4}$	0	64
CIFAR100	CNN	20000	5	1	10^{-2}	$4 \cdot 10^{-4}$	0	64
	ResNet18-GN	10000	10	1	10^{-2}	10^{-5}	0.7	64
LANDMARKS-USER-160K	MobileNetv2	1300	50	5	0.1	$4 \cdot 10^{-5}$	0	64

Table 15. Search grid used to find optimal hyper-parameters for each combination of method, dataset and model. We highlight the best performing values in **bold**.

Method	HParam	CIFAR10		CIFAR100		LANDMARKS-USER-160K
		CNN	ResNet18	CNN	ResNet18	
FEDSAM	ρ	[0.05, 0.1, **0.15**, 0.2]	[**0.01**, 0.02, 0.05]	[0.005, **0.01**, 0.02, 0.05]	[**0.01**, 0.02, 0.05]	[**0.05**]
FEDPROX	μ	[0.001, 0.01, **0.1**]	[0.001, **0.01**, 0.1]	[0.001, 0.01, **0.1**]	[0.001, 0.01, **0.1**]	[0.001, 0.01, **0.1**]
FEDDYN	α	[0.001, **0.01**, 0.1]	[0.001, **0.01**, 0.1]	[0.001, **0.01**, 0.1]	[**0.01**]	[**0.001**, 0.01]
	ρ (SAM-based only)	[**0.15**]	[**0.01**]	[0.01, **0.02**]	[**0.01**]	[**0.05**]
FEDSPEED	ρ	[0.05, 0.1, **0.15**, 0.2]	[**0.01**]	[0.005, **0.01**, 0.02, 0.05]	[**0.01**]	[**0.05**]
	α	[0.9, **0.95**, 0.99]	[0.9, **0.95**]	[0.9, **0.95**, 0.99]	[0.9, **0.95**]	[**0.95**]
	λ	[10, **100**, 1000]	[10, 100, **1000**]	[10, 100, **1000**]	[10, 100, **1000**]	[100, **1000**]
FEDGAMMA	ρ	[**0.15**]	[**0.01**]	[**0.01**]	[**0.01**]	[**0.05**]
FEDSMOO	ρ	[0.05, 0.1, **0.15**, 0.2]	[**0.01**]	[0.005, 0.01, 0.05, **0.1**, 0.2]	[**0.01**]	[0.05, **0.1**, 0.2, 0.3]
	β	[5, **10**, 100]	[1, 2, **5**, 10]	[10, **100**]	[5, **10**, 100]	[10, **50**, 100, 1000]
FEDGLOSS (ours)	ρ_s	[0.01, 0.1, **0.15**]	[**0.01**, 0.05, 0.1, 0.5]	[**0.01**, 0.05, 0.1, 0.2]	[**0.01**, 0.05, 0.1, 0.5]	[**0.005**, 0.01, 0.02]
	ρ	[0.05, 0.1, **0.15**, 0.2]	[**0.01**]	[0.05, 0.1, **0.2**]	[**0.01**]	[0.05, 0.1, 0.2, **0.3**]
	β	[5, **10**, 100]	[**1**, 2, 5, 10]	[10, **100**]	[**5**, 10, 100]	[10, **50**, 100]
	T_s	[1000, **2000**, 4000]	[**0**]	[1000, 2000, 5000, 10000, **15000**]	[**0**]	[**0**]

D.1. Visualizing 3D Loss Landscapes

We leverage techniques from [31] to visualize the loss landscapes of our models. We adapt their code to work with our specific datasets and network architectures. The process involves calculating the loss function along random directions in the parameter space. This is achieved by perturbing the model's parameters within a defined range. In our visualizations, we constrain these perturbations to occur within the range of $[-1, 1]$ for both the x and y axes. To ensure consistent comparisons across models (*e.g.*, as seen in Fig. 6), we utilize the same set of random directions for all models.

D.2. Visualizing 1D Loss Landscapes

Fig. 19 shows the interpolation of FEDGLOSS and NAIVEFEDGLOSS's models. Given their respective weights $\boldsymbol{w}_{\text{FEDGLOSS}}$ and $\boldsymbol{w}_{\text{NAIVEFEDGLOSS}}$, the interpolation is computed using a coefficient γ as

$$\boldsymbol{w} = \gamma \cdot \boldsymbol{w}_{\text{FEDGLOSS}} + (1 - \gamma) \cdot \boldsymbol{w}_{\text{NAIVEFEDGLOSS}} \,. \tag{8}$$

For each $\gamma \in [-1, 2]$, $\boldsymbol{w}$ is tested on the training or test sets, and the plot reports the computed loss. The resulting interpolation indicates that there is no loss barrier between the two models, suggesting they lie within the same basin. Additionally, the 1D geometry of the emerging loss landscape reveals that both models converge to a flat minimum when evaluated on both CIFAR100 and CIFAR10.

D.3. Hessian Eigenvalues for Flatness Measure

Following prior work [4, 12, 14, 31], we use the spectrum of the Hessian matrix to quantify the *flatness* of the loss landscape. Here, lower maximum eigenvalues correspond to flatter landscapes, implying less sharpness. To compute these eigenvalues (denoted by λ_1 in the main paper), we employ the stochastic power iteration method [60] with a maximum of 20 iterations, referring to the code of Golmant et al. [15].